

We sincerely thank the reviewer for the comments, which helped us to improve our manuscript. Please find the comments (blue) and our reply (black) below.

#### General comments

The article “Greenhouse gas production in degrading ice-rich permafrost deposits in northeast Siberia” by Josefine Walz et al. discusses the important issue of permafrost aggradation history and organic matter quality on greenhouse gas (CO<sub>2</sub> and CH<sub>4</sub>) production from degrading yedoma deposits. The findings are based on short-term (134 days) and longer-term (785 days) incubation of samples collected at three locations, and the measured CO<sub>2</sub> and CH<sub>4</sub> production is linked to a wide array of measurements on geochemical characteristics and the stratigraphy of soil/sediment cores.

The potential future C release from thawing permafrost soils, especially yedoma, is connected to large uncertainties. Only a limited number of studies address this topic and I particularly value the authors' efforts to assess the longer-term production potential. This topic clearly is of interest to the broader scientific community and I thus consider this manuscript highly relevant for the journal. The manuscript is carefully written, however, it would benefit from some streamlining, especially of the results and discussion section as outlined in my comments below, in order to further improve readability and scientific value of the manuscript.

#### Specific comments

1) First of all, the results section is rather detailed, partly repeating values presented as figures and reporting many numbers, making it difficult to follow. I would recommend providing part of the information as tables, e.g. an overview table with site names, site codes, ages, mean CO<sub>2</sub> and CH<sub>4</sub> production rates etc., helping the reader to get an overview of the differences between the three locations.

We added Tabel 2 as a summary table as suggested and removed some of the detailed numbers from the results section to improve readability.

Chapters 4.2, 4.3, 4.4 should be presented under a sub-heading, e.g. “greenhouse gas production”.

Chapters 4.2, 4.3, 4.4 are now presented under the sub-heading, “Greenhouse gas production potentials” as suggested.

To improve readability, I would further recommend dropping the numbers in the site codes, e.g. just MUO, BK, and L instead of MUO12, BK8, L14.

We decided to keep the numbers in the site codes, because the same numbers and codes were used for the same sample material in other studies that are referenced in this study. Hence, keeping codes and numbers facilitates the comparison of data from different studies.

2) the conclusions drawn in the discussions are partly based on results obtained in this study, but also quite heavily rely on detailed analyses reported in previously published literature (radiocarbon age, plant macrofossils and soil microbial analyses), e.g. L285-303. I suggest to emphasize results measured within this study throughout the discussion. Additionally, section 5.1 of the discussion is rather lengthy and would benefit from some streamlining to more clearly emphasize the main results from this study.

We rewrote parts of Section 5.1 and 5.2 to shorten and streamline the discussion and to put more emphasis on the incubation results of this study, see. lines 285–299, lines 319–320, or 359–363.

3) The CO<sub>2</sub> and CH<sub>4</sub> production potential was assessed using separately incubated soil samples, excluding effects of vegetation (e.g. input of fresh OM to the soil system, atmospheric CO<sub>2</sub> uptake), and processes among different layers in the soil profile (e.g. diffusion and leaching, as well as priming of old OM). How would the authors relate the gas production measured in these soil incubations to gas release to the atmosphere under in situ conditions? I would appreciate some more discussion on this part.

Post-thaw processes and the introduction of fresh organic are important points. We included some discussion of the priming effects on organic matter decomposability in section 5.1, L307-312.

#### Technical corrections / line edits

**Abstract L31: if more than 80% were produced during the first 134 of the long-term incubation, shouldn't that rather highlight the importance of the labile C pool, rather than the slowly decomposing C pool?**

Yes, the labile pool is important for the production in the initial incubation. But this pool is very small. So over longer time scales, the slowly decomposing C pool will become relevant. In the abstract we now refer to the non-linearity of the decomposition processes and discuss the importance of fast vs slowly decomposing C in the discussion.

**Introduction L40: give depth range for C stocks, is it 0-3m?**

This is the combined C stock of soils, refrozen thermokarst and Holocene cover deposits in the top 3 m as well as sediments and deltaic deposits below 3 m. We added this information in the text for clarity.

**L44: "The changes" is slightly vague, please specify.**

We replaced "The changes" with "The effects of elevated atmospheric greenhouse gas concentrations and temperatures on processes in soils and sediments".

**L54: what about MIS 4 and 6, are they not preserved in this region?**

MIS4 deposits are preserved in the region, but not all MIS 4 deposits are ice complex deposits, e.g. in the Kuchchugui Suite on Bol'shoy Lyakhovsky. In the text, we added the information, that "at some locations the accumulation of Yedoma material may have already started between 80 and 60 ka BP, i.e. during MIS 4" (L 55–56). Dating constraints of older, non-yedoma ice complexes, make it difficult to differentiate if the deposition occurred during the MIS7 or early MIS 6. In the text, we added the possibility of ice complex formation during both late MIS 7/early MIS 6 and MIS 5 (L57-59).

**L60: Either separate sentence by colon ":" or add reference.**

We added a reference.

**L62-64: Are those C stocks representative of the whole yedoma deposits, or a certain depth range?**

Those C stocks are for the whole Yedoma domain. We clarified this in the text.

**L66: Consider replacing "thawed out", e.g. "exposed by degradation of ice-rich permafrost"**

We changed "is thawed out from degrading ice-rich permafrost deposits" to "will be exposed by degradation of ice-rich permafrost" as suggested.

**L67: decomposed to the greenhouse gases carbon dioxide (CO<sub>2</sub>) and methane (CH<sub>4</sub>)**

We changed the sentence as suggested.

**L77: Do they authors mean "permafrost aggradation"?**

Yes. We corrected this typo.

**Methods L97: Consider replacing "modern" with "current"**

We replaced "modern" with "current" as suggested.

**L155: Might the low temperatures during storage (-18oC) have had an effect on soil microbial community functioning during the incubations? -11oC seems to be the minimum naturally occurring permafrost temperature in this region.**

We do not expect that the storage temperature will considerably affect the soil microbial community functioning because -11 °C is the ground temperature at the level of zero amplitude, which is at about 20 meters depth. Above that point, temperatures will be lower in winter, with colder temperatures in the upper permafrost and the coldest temperatures in the active layer reaching values of below -30°C.

**L164/165:**

**Some specifications about the gas sampling would be useful, e.g. how many mL of gas were sampled from the headspace for GC analysis? Did gas sampling cause underpressure in the headspace?**

We always worked with slight overpressure. In individual cases of underpressure, which occasionally occurred in the longer incubations, we added 5-10 mL of N<sub>2</sub> gas to reestablish overpressure in the bottle. We removed 1 mL of headspace gas for each individual GC measurement and corrected for the cumulative removed gas during sampling. We added this information in the Section 3.3.

L171-174: Was the temperature dependency of gas solubility taken into account? I would suggest to provide some more details on the solubility/temperature coefficients used for CO<sub>2</sub> and CH<sub>4</sub>.

Carroll et al. (1991) and Yamamoto et al. (1976) provide temperature-dependent solubility for CO<sub>2</sub> and CH<sub>4</sub>, respectively. In the text, we added the information "Solubility for CO<sub>2</sub> and CH<sub>4</sub> in water at 4 °C".

Results L236: "anaerobic CO<sub>2</sub> production"?

Yes. We added "production"

L243: increased 30-fold over what time frame?

We added the "between 134 and 785 incubation days".

Discussion L282-284: This seems like an overall conclusion of the study and does not belong in the opening paragraph of the discussion

We moved this sentence to the conclusion section and replaced it here with a more appropriate introductory sentence.

L369-372: Using the term "longterm" for a period of ca. 2 years is slightly questionable, I advise some caution with the use of this term throughout the manuscript.

Were appropriate, we replaced "long-term" throughout the text.

Figures L675 (Fig. 3): adding both y-axes (height and depth) to each figure panel, as well as using the same x-axis scaling (e.g. 0-80?) would improve readability of the figure. Since CH<sub>4</sub> production is included as a third panel for the other cores, please mention in figure caption why it is not included here. L684 (Fig. 4 and Fig. 5): Please mention AL thickness in figure caption.

We tried adding both y-axes to each figure panel in Fig. 3, 4, and 5, but this made the figures overly busy, so we decided to keep the y-axes as is. We added the AL thickness in figure captions 4 and 5.

Cited references:

Carroll, J. J., Slupsky, J. D. and Mather, A. E.: The solubility of carbon dioxide in water at low pressure, J. Phys. Chem. Ref. Data, 20(6), 1201, doi:10.1063/1.555900, 1991.

Yamamoto, S., Alcauskas, J. B. and Crozier, T. E.: Solubility of methane in distilled water and seawater, J. Chem. Eng. Data, 21(1), 78–80, doi:10.1021/je60068a029, 1976.

Thank you for the helpful suggestions on this manuscript. Please find the comments (blue) and our reply (black) below.

Authors using the word "glacial" very often do not specify that they mean age but not the origin of the deposits they studied. It might confuse the readers who are not familiar with the paleoenvironmental conditions of the area of investigation. I suggest to use marine isotopic stages or regional stratigraphic units.

Where necessary, we changed "glacial" to refer only to age and not origin to avoid ambiguity, e.g. line 23 and line 274.

Lines 64 and 65. I would recommend to authors include in the review of the assessments of the carbon pools in different stratigraphic horizons research published by Shmelev et al (Shmelev, D., Veremeeva, A., Kraev, G., Kholodov, A., Spencer, R. G., Walker, W. S., & Rivkina, E. (2017). Estimation and Sensitivity of Carbon Storage in Permafrost of North-Eastern Yakutia. *Permafrost and Periglacial Processes*, 28(2), 379-390.).

We included this information as suggested in lines 69–72.

Line 95. It is not so important for this study, but permafrost temperature in this region varies with the topographic forms and consist of -9 within the thermokarst depressions and -10.5 at the yedoma hills (Kholodov, A., Gilichinsky, D., Ostroumov, V., Sorokovikov, V., Abramov, A., Davydov, S., & Romanovsky, V. (2012, June). Regional and local variability of modern natural changes in permafrost temperature in the Yakutian coastal lowlands, Northeastern Siberia. In *Proceedings of the Tenth International Conference on Permafrost, Salekhard, Yamal-Nenets Autonomous District, Russia* (pp. 25-29).)

Thank you for this reference. However, we agree that the temperature differences between topographic forms are not of utmost importance for the current study.

For the Results section, I also recommend authors to insert the graphs of dynamics of the greenhouse gases production during the experiment to give readers a better idea about dynamics of the process of organic matter decay.

Thank you for this important comment. We will deposit all the data of the current manuscript on PANGAEA (<https://doi.pangaea.de/10.1594/PANGAEA.892950>) so we decided not to insert the graphs of dynamics of the greenhouse gas production during the incubation of the samples in the manuscript. Since we incubated 117 individual samples, this cannot be done in a reasonable way.

Please find below a list of all relevant changes made in the manuscript:

- We added Table 2 as a summary table and removed some of the detailed numbers from the results section to improve readability.
- Chapters 4.2, 4.3, 4.4 are now presented under the sub-heading, “Greenhouse gas production potentials”
- We rewrote parts of Section 5.1 and 5.2 to shorten and streamline the discussion and to put more emphasis on the incubation results of this study, see. lines 285–299, lines 319–320, or 359–363.
- We included some discussion of the priming effects on organic matter decomposability in section 5.1, lines 307-312.
- We added details about ice complex formation in lines 55-59.
- We added details about the incubation procedure in Section 3.2, lines 161-164.
- Where necessary, we changed “glacial” to refer only to age and not origin to avoid ambiguity, e.g. line 23 and line 274.
- We added information about carbon pools in lines 69–72.
- We deposited all data of the current manuscript on PANGAEA (<https://doi.pangaea.de/10.1594/PANGAEA.892950>) and added this reference

# 1 Greenhouse gas production in degrading ice-rich permafrost deposits in northeast Siberia

2 Josefine Walz<sup>1,2</sup>, Christian Knoblauch<sup>1,2</sup>, Ronja Tigges<sup>1</sup>, Thomas Opel<sup>3,4</sup>, Lutz Schirrmeister<sup>4</sup>, Eva-Maria  
3 Pfeiffer<sup>1,2</sup>

4  
5 <sup>1</sup>Institute of Soil Science, Universität Hamburg, Hamburg, 20146, Germany

6 <sup>2</sup>Center for Earth System Research and Sustainability, Universität Hamburg, Hamburg, 20146, Germany

7 <sup>3</sup>Permafrost Laboratory, Department of Geography, University of Sussex, Brighton, BN1 9RH, UK

8 <sup>4</sup>Alfred Wegener Institute Helmholtz Centre for Polar and Marine Research, ~~Periglacial Permafrost~~  
9 ~~Research Section~~, 14473 Potsdam, Germany

10 *Correspondence to:* Josefine Walz ([josefine.walz@uni-hamburg.de](mailto:josefine.walz@uni-hamburg.de))

11

## 12 Abstract

13 Permafrost deposits have been a sink for atmospheric carbon for millennia. Thaw-erosional processes,  
14 however, can lead to rapid degradation of ice-rich permafrost and the release of substantial amounts of  
15 organic carbon (OC). The amount of the OC stored in these deposits and their potential to be microbially  
16 decomposed to the greenhouse gases carbon dioxide (CO<sub>2</sub>) and methane (CH<sub>4</sub>) depends on climatic  
17 and environmental conditions during deposition and the decomposition history before incorporation into  
18 the permafrost. Here, we examine potential greenhouse gas production in degrading ice-rich permafrost  
19 deposits from three locations in the northeast Siberian Laptev Sea region. The deposits span a period  
20 of about 55 kyr ~~and include deposits~~ from the last glacial period and Holocene interglacial ~~periods~~.  
21 Samples from all three locations were incubated under aerobically and ~~anaerobically incubated~~  
22 conditions for 134 days at 4 °C. Greenhouse gas production was generally higher in deposits from glacial  
23 periods, where 0.2–6.1% of the initially available OC was decomposed to CO<sub>2</sub>. glacial than Holocene  
24 deposits. In contrast, only 0.1–4.0% of initial OC in permafrost deposits from the were decomposed in  
25 permafrost deposits from the Holocene and the late glacial transition, ~~only 0.1–4.0% of the initially~~  
26 ~~available OC could be decomposed to CO<sub>2</sub>, while 0.2–6.1% could be decomposed in glacial deposits.~~  
27 Within the glacial deposits from the Kargin interstadial period (Marine Isotope Stage 3), local depositional  
28 environments, especially soil moisture, also affected the preservation of OC. Sediments deposited under  
29 wet conditions contained more labile OC and thus produced more greenhouse gases than sediments  
30 deposited under drier conditions. To assess the long-term greenhouse gas production potentials over  
31 longer periods, deposits from two locations were incubated for a total of 785 days. However, more than

32 50% of total CO<sub>2</sub> production over 785 days occurred within the first 134 days under aerobic conditions  
33 while even 80% were produced over the same period under anaerobic conditions, which emphasizes  
34 the non-linearity of the OC decomposition processes~~of the aerobically produced and more than 80% of~~  
35 ~~anaerobically produced CO<sub>2</sub> after 785 days of incubation were already produced within the first 134 days,~~  
36 emphasizing the non-linearity of the decomposition processes. ~~highlighting the quantitative importance~~  
37 ~~of the slowly decomposing OC pool in permafrost.~~ CH<sub>4</sub> production Methanogenesis was generally  
38 observed in active layer samples but only sporadically in permafrost samples and was several orders of  
39 magnitude smaller than CO<sub>2</sub> production.

40

41 Key words: Permafrost ~~carbon~~thaw, ~~greenhouse gases~~CO<sub>2</sub> and CH<sub>4</sub>, incubation, Yedoma, Siberian  
42 Arctic

43

## 44 **1 Introduction**

45 Permafrost, i.e. ground that is at or below  $\leq 0$  °C for at least two consecutive years (van Everdingen,  
46 2005), may preserve organic matter (OM) for millennia (Ping et al., 2015). The current organic carbon  
47 (OC) pool of ~~soils and sediments in permafrost-affected landscapes,~~ soils, refrozen thermokarst, and  
48 Holocene cover deposits in the top 3 m as well as sediments and deltaic deposits below 3 m in permafrost  
49 landscapes is estimated to be about ~1300 Pg, of which about ~800 Pg are perennially frozen (Hugelius  
50 et al., 2014). However, warming-induced environmental changes and permafrost degradation could lead  
51 to rapid thaw of substantial amounts of currently frozen OM, microbial decomposition of the thawed  
52 ~~material~~OM, and rising greenhouse gas fluxes to the atmosphere (Natali et al., 2015; Schuur et al., 2015).  
53 The ~~changes~~ effects of elevated atmospheric greenhouse gas concentrations and temperatures on  
54 processes in soils and sediments are expected to be most pronounced in near-surface layers (Schneider  
55 von Deimling et al., 2012). However, ~~but~~ thermo-erosion of ice-rich permafrost, i.e. permafrost with  
56 >more than 20 vol% ice (Brown et al., 1998), also enables deep thaw of several tens of meters  
57 (Schneider von Deimling et al., 2015).

58 Ice-rich permafrost deposits, also called ice complex deposits, accumulated in unglaciated Arctic  
59 lowlands. During cold stages, fine grained organic-rich material of polygenetic origin was deposited on  
60 predominantly flat plains (Schirrmeister et al., 2013). The deposits are dissected by large ice wedges,  
61 which can amount for up to 60 vol% (Ulrich et al., 2014). The most prominent ice complex deposits,  
62 referred to as Yedoma, accumulated during the late Pleistocene between >approximately 55 and 13 ka

63 before present (BP), i.e. during the Marine Isotope Stages (MIS) 3 and 2 (Schirrmeister et al., 2011).  
64 Age-depth correlations, however, indicate that at some locations the accumulation of Yedoma material  
65 may have already started between 80– and 60 ka BP, i.e. during MIS 4. (Schirrmeister et al., 2002b).  
66 Locally, ~~however,~~ remnants of older ice complex deposits of both late MIS 7/early MIS 6 ~~or~~ and MIS 5  
67 age are also preserved (Opel et al., 2017; Schirrmeister et al., 2002a; Wetterich et al., 2016), but not  
68 studied yet in terms of greenhouse gas production.

69 The thickness of Yedoma deposits in Siberia (Grosse et al., 2013) and Alaska (Kanevskiy et al., 2011)  
70 can reach more than >50 m. At the time of deposition; rapid sedimentation and freezing incorporated  
71 relatively undecomposed OM into the permafrost (Strauss et al., 2017). However, owing to the high ice  
72 content, Yedoma deposits are highly susceptible to warming-induced environmental changes, erosion,  
73 and ground subsidence following permafrost thaw (e.g. Morgenstern et al., 2013). Only 30% of the  
74 Yedoma region (about ~416,000 km<sup>2</sup>) is considered intact, ~~(Strauss et al., 2013)~~ while the other 70%  
75 have already undergone some level of permafrost degradation (Strauss et al., 2013) ~~(e.g. Morgenstern~~  
76 ~~et al., 2013)~~. Today, the whole Yedoma region-domain stores 213–456 Pg of OC, of which 83–269 Pg  
77 are stored in intact Yedoma and 169–240 Pg in thermokarst and refrozen taberal deposits (Hugelius et  
78 al., 2014; Strauss et al., 2013, 2017; Walter Anthony et al., 2014; Zimov et al., 2006). For an about  
79 88,000 km<sup>2</sup> large area along the Bolshaya Chukochya and Alazeya Rr ~~R~~ river basins and the eastern parts  
80 of the Yana-Indigirka and Kolyma lowlands in northeast Siberia, Shmelev et al. (2017), estimate the size  
81 of the total carbon pool in the upper 25 m to be 31.2 Pg, of which 3.7 Pg are stored in Yedoma deposits.  
82 ~~But~~ However, high spatial and temporal variability result in large uncertainties about ~~of~~ how much OC will  
83 be exposed by degradation of ice-rich permafrost is thawed out from degrading ice-rich permafrost  
84 deposits and how much of this OC can be microbially decomposed to the greenhouse gases carbon  
85 dioxide (CO<sub>2</sub>) or methane (CH<sub>4</sub>) after thaw.

86 In addition to the quantity of OCM, its decomposability will influence how fast the OC in Yedoma  
87 permafrost deposits can be transformed into CO<sub>2</sub> or CH<sub>4</sub> after thaw (Knoblauch et al., 2018; MacDougall  
88 and Knutti, 2016). Since plants are the main source of OM in soils, vegetation composition plays an  
89 important role for OM decomposability (Iversen et al., 2015). Furthermore, OM has undergone different  
90 degradation processes before being incorporated into permafrost depending on permafrost formation  
91 pathways (Harden et al., 2012; Waldrop et al., 2010). In epigenetic permafrost, that is permafrost  
92 aggradation through intermittent freezing after the material was deposited, OM has already undergone  
93 some level of transformation and easily decomposable, labile OC compounds are decomposed and lost

94 to the atmosphere prior to incorporation into the permafrost (Hugelius et al., 2012). In contrast, OM in  
95 syngenetically frozen Yedoma, i.e. concurrent material deposition and permafrost  
96 ~~aggradation~~aggregation, had little time to be transformed prior to freezing and may thus contain high  
97 amounts of labile OCM, which may be quickly decomposed to greenhouse gases after thaw (Dutta et  
98 al., 2006). In this case, the amount and decomposability of the fossil OM is controlled by the OM source,  
99 i.e. predominantly vegetation, which in turn depends on paleo-climatic conditions (Andreev et al., 2011).

100 The decomposability of permafrost OM is often assessed based on OM degradation proxies, total OC  
101 (TOC) content, total organic carbon to- total nitrogen ratios (C/N), or stable carbon isotopes ( $\delta^{13}\text{C}_{\text{org}}$ ) with  
102 contradictory results (Strauss et al., 2015; Weiss et al., 2016). Only few studies have measured  $\text{CO}_2$  and  
103  $\text{CH}_4$  production potentials from Siberian Yedoma deposits under laboratory conditions (Dutta et al., 2006;  
104 Knoblauch et al., 2013, 2018; Lee et al., 2012; Zimov et al., 2006). In this study, we present incubation  
105 data from late Pleistocene Yedoma and Holocene interglacial deposits from three locations in northeast  
106 Siberia. We hypothesize that OM deposited during glacial periods experienced little pre-freezing  
107 transformation and thus provides a more suitable substrate for future microbial decomposition and  
108 greenhouse gas production post-thawing than Holocene deposits.

109

## 110 **2 Study region and sample material**

111 Three locations in the Laptev Sea region in northeast Siberia were studied (Fig. 1). The whole region is  
112 underlain by continuous permafrost reaching depths of 450–700 m onshore and 200–600 m offshore  
113 (Romanovskii et al., 2004) with ground temperatures of  $-11\text{ }^\circ\text{C}$  for terrestrial permafrost (Drozdov et al.,  
114 2005) and  $-1\text{ }^\circ\text{C}$  for submarine permafrost (Overduin et al., 2015). Long, cold winters and short, cool  
115 summers characterize the ~~modern-current~~ climate. Mean annual (1971–2000) temperatures and  
116 precipitation sums are  $-13.3\text{ }^\circ\text{C}$  and 266 mm at the central Laptev Sea coast (Tiksi, WMO station 21824)  
117 and  $-14.9\text{ }^\circ\text{C}$  and 145 mm in the eastern Laptev Sea region (Mys Shalaurova, WMO station 21647,  
118 Bulygina and Razuvaev, 2012). Modern vegetation cover is dominated by erect dwarf-shrub and in  
119 places by sedge, moss, low-shrub wetland vegetation or tussock-sedge, dwarf-shrub, moss tundra  
120 vegetation (CAVM Team, 2003). A compilation of the regional stratigraphic scheme used in this work  
121 with paleoclimate and vegetation history is summarized in Table 1.

122 The first study location is on Muostakh Island ( $71.61^\circ\text{ N}$ ,  $129.96^\circ\text{ E}$ ), an island in the Buor Khaya Bay  
123 40 km east of Tiksi. Between 1951–2013, the area and volume of Muostakh Island, which is subject to  
124 major coastal erosion (up to  $-17\text{ m a}^{-1}$ ) and thaw subsidence, decreased by 24% and 40%, respectively

125 (Günther et al., 2015). The entire sedimentary sequence of Muostakh Island (sample code MUO12) was  
126 sampled in three vertical sub-profiles on the northeastern shore (Meyer et al., 2015). In the current study,  
127 we used 14 sediment samples from the entire MUO12 sequence between 0.5–15.6 meters below surface  
128 (mbs), which corresponds to 19.5–4.4 meters above sea level (masl).

129 The second study location is on the Buor Khaya Peninsula (71.42° N, 132.11° E). Thermokarst  
130 processes affect 85% of the region, which resulted in [more than](#) >20 m of permafrost subsidence in some  
131 areas (Günther et al., 2013). Long-term (1969–2010) coastal erosion rates along the western coast of  
132 the Buor Khaya Peninsula are ~~about~~ [-1 m a<sup>-1</sup>](#) (Günther et al., 2013). On top of the Yedoma hill,  
133 approximately 100 m from the cliff edge, a 19.8 m long permafrost core (sample code BK8) was drilled  
134 (Grigoriev et al., 2013). Detailed cryolithological, geochemical, and geochronological data (Schirrmeister  
135 et al., 2017), palynological analysis (Zimmermann et al., 2017b), and lipid biomarker studies (Stapel et  
136 al., 2016) were previously published for the BK8 site. In the current study, 20 sediment samples spread  
137 evenly between the surface and 19.8 mbs (or ~~34 to~~ [14.2 masl](#)) were analyzed, excluding an ice wedge  
138 between 3.2–8.5 mbs.

139 The third sampling location is on Bol'shoy Lyakhovsky Island (73.34° N; 141.33° E), the southernmost  
140 island of the New Siberian Archipelago. Four cores (sample code L14) were drilled on the southern coast  
141 (Schwamborn and Schirrmeister, 2015). Core descriptions, [geochronological data as well as, and](#) pollen  
142 and plant DNA analyses can be found in Zimmermann et al. (2017a), while biomarkers and pore water  
143 analysis [can be found are reported](#) in Stapel et al. (2018). Based on previous stratigraphic studies from  
144 this location (e.g. Andreev et al., 2009; Wetterich et al., 2009, 2014) we focused on two cores, which  
145 represent the here investigated MIS 1–MIS 3 period. The first core, L14-05, was recovered from inside  
146 a thermokarst basin, 4 km west of the Zimov'e River mouth, with Holocene thermokarst deposits  
147 overlying thawed and refrozen taberal Yedoma deposits (Wetterich et al., 2009). Five sediment samples  
148 between 0–7.9 mbs (11.5–3.6 masl) were analyzed for the current study. The second core, L14-02, was  
149 taken on a Yedoma hill about 1 km west of the Zimov'e River mouth. The entire core was 20.0 m long,  
150 including wedge ice below 10.9 mbs. Five sediment samples from the top to a depth of 10.9 mbs (32.2–  
151 21.3 masl) were incubated for the current study.

152

## 153 **3 Methods**

### 154 **3.1. Dating**

155 ~~Radiocarbon dating was performed on plant macro fossils for MUO12 (Meyer et al., unpublished data),~~  
156 ~~BK8 (Schirrmeister et al., 2017), and L14 samples (Zimmermann et al., 2017a) using the AMS facilities~~  
157 ~~of University of Poznan and Cologne University. Additionally, feldspars grains from the BK8 core at 12.6–~~  
158 ~~12.75 mbs, 16.0–16.35 mbs 18.5–18.7 mbs were dated by infrared-stimulated luminescence (IRSL)~~  
159 ~~(Schirrmeister et al., 2017).~~

160

### 161 **3.2.3.1. Geochemical characteristics**

162 Gravimetric water contents were calculated as the weight difference between wet and dried (105 °C)  
163 samples. pH values were measured in a suspension of 5 g thawed sediment in 12.5 ml distilled water  
164 (CG820, Schott AG, Mainz, Germany). For sediment chemical analyses, bulk samples were dried at  
165 70°C and milled. Total carbon (TC) and total nitrogen (TN) contents were measured with an element  
166 analyzer (VarioMAX cube, Elementar Analysensysteme GmbH, Hanau, Germany), while TOC contents  
167 were measured with a liquiTOC II coupled to a solids module (Elementar Analysensysteme GmbH,  
168 Hanau, Germany). The  $\delta^{13}\text{C}_{\text{org}}$ -values were measured with an isotope-ratio mass spectrometer (Delta V,  
169 Thermo Scientific, Dreieich, Germany) coupled to an elemental analyzer (Flash 2000, Thermo Scientific,  
170 Dreieich, Germany) after samples were treated with phosphoric acid to release inorganic carbon.

171

### 172 **3.3.3.2. Incubation**

173 Frozen samples were slowly thawed from -18 °C to 4 °C over 48 h in a refrigerator, ~~and~~ homogenized  
174 ~~and divided into triplicates~~. Anaerobic incubations were prepared under a nitrogen atmosphere in a glove  
175 box. Approximately 15–30 g thawed sediment was weighed into glass bottles and sealed with rubber  
176 stoppers. Anaerobic samples were saturated with 5–20 ml of nitrogen-flushed, CO<sub>2</sub>-free distilled water  
177 and the headspace was exchanged with molecular nitrogen. The headspace of aerobic incubation bottles  
178 was exchanged with synthetic air (20% oxygen, 80% nitrogen). We added enough molecular nitrogen  
179 and synthetic air to establish a slight overpressure inside each bottle. In occasional cases of negative  
180 pressure differences between headspace pressure and underpressure ambient pressure, inside a bottle  
181 over the course of the incubation, we added 5–10 mL of molecular nitrogen to reestablish overpressure.

182 Samples from all three study locations were incubated for 134 ~~incubations~~ days at 4 °C. During this  
183 time, the headspace CO<sub>2</sub> and CH<sub>4</sub> concentrations were measured weekly to biweekly. The incubation of

184 samples from the Buor Khaya Peninsula and Bol'shoy Lyakhovsky Island continued until 785 days and  
185 the gas concentrations were measured. ~~The measuring intervals gradually decreased to~~ every 8–12  
186 weeks ~~for the remaining incubation period~~. To determine the gas concentrations inside each bottle, 1  
187 mL of headspace gas was removed by a syringe and injected into a ~~were determined by a~~ gas  
188 chromatograph (GC 7890 Agilent Technologies, Santa Clara, USA) equipped with a 500 µL sample loop,  
189 a nickel catalyst to reduce CO<sub>2</sub> to CH<sub>4</sub>, and a flame ionizing detector (FID). Gases were separated on a  
190 PorapakQ column with helium as carrier gas. If the headspace concentration of CO<sub>2</sub> in aerobic incubation  
191 bottles approached 3%, the headspace was again exchanged with synthetic air.

192 The amount of gas in the headspace was calculated from the concentration in the headspace,  
193 headspace volume, incubation temperature, and pressure inside the bottle using the ideal gas law. The  
194 amount of gas dissolved in water was calculated from the gas concentration in the headspace, pressure  
195 inside the bottle, water content, pH, and gas solubility. Solubility for CO<sub>2</sub> and CH<sub>4</sub> in water at 4 °C was  
196 calculated after Carroll et al. (1991) and Yamamoto et al. (1976), respectively. To account for the  
197 dissociation of carbonic acid in water at different pH values, we used dissociation constants from Millero  
198 et al. (2007).

199

### 200 3.4.3.3. **Statistics**

201 Differences in mean values were analyzed with the Kruskal-Wallis test followed by multiple post-hoc  
202 Mann-Whitney tests with Bonferroni adjustment for multiple group comparisons. We tested for  
203 differences between deposits from different periods as well as for differences between deposits from the  
204 same period but from different locations. In both cases, the number of post-hoc comparisons was three,  
205 giving an adjusted significance level of 0.017. All statistical analyses were performed using MATLAB®  
206 (MATLAB and Statistics Toolbox Release 2015b, The MathWorks Inc., Natick, MA, USA).

207

## 208 **4 Results**

### 209 **4.1. Chronostratigraphy and geochemical characteristics**

210 The sedimentary sequence on Muostakh Island was divided into three sections, which were separated  
211 by two erosional contacts and sharply intersecting ice wedges (Meyer et al., 2015). Based on radiocarbon  
212 ages (Meyer et al., unpublished data), these sections could be separated into three periods (Fig. 3).  
213 Deposits from the uppermost section between 0.5–2.4 mbs were classified as Holocene deposits from  
214 the MIS 1 and deposits from the late glacial to early Holocene transition, confirmed by radiocarbon ages

215 of 7.5 and 13.2 ka BP for samples at 1.3 and 2.4 mbs, respectively. The middle section between 4–10  
216 mbs yielded radiocarbon ages of 16.1–18.9 ka BP and were therefore classified as Sartan stadial  
217 deposits from the MIS 2. The lowermost section between 11.3–15.6 mbs yielded radiocarbon ages of  
218 41.6–45.9 ka BP and represents the MIS 3 Kargin interstadial.

219 The BK8 core from the Buor Khaya Peninsula was subdivided into four sections (Fig. 4). The first  
220 section between 0–0.5 mbs represents the seasonally thawed active layer. The subdivision of the  
221 permafrost deposits below the active layer was based on previously published radiocarbon and [infrared-](#)  
222 [stimulated luminescence \(IRSL\)](#) ages (Schirrmeister et al., 2017). Deposits from the second section  
223 between 0.5–3.2 mbs yielded radiocarbon ages between 9.7–11.4 ka BP, which corresponds to the late  
224 glacial transition to the early Holocene. The third section between 3.2–8.5 mbs consisted of an ice  
225 wedge, which was not sampled for the current study. The fourth section between 8.5–18.9 mbs yielded  
226 infinite radiocarbon ages [of >older than](#) 50 ka BP. The additional IRSL ages of feldspar grains yielded  
227 deposition ages of [about](#) ~45 ka BP. Thus, sediments from this section were classified as deposits from  
228 the Kargin interstadial.

229 The upper 0.5 m from both cores from Bol'shoy Lyakhovsky Island represent the active layer.  
230 Radiocarbon ages of the L14-05 core from the thermokarst basin ranged between 2.2–10.1 ka BP for  
231 the upper core section between 0–1.7 mbs and 51.2–54.6 ka BP for deposits below 5.8 mbs  
232 (Zimmermann et al., 2017a). Based on these ages, stratigraphic interpretations from a nearby outcrop  
233 (Wetterich et al., 2009) and the available palynological data (Zimmermann et al., 2017a), the L14-05  
234 core was divided into two parts (Fig. 5). The upper part between 0–5.5 mbs were deposited during the  
235 Holocene and late glacial transition, while deposits below 5.5 mbs [was deposited during originate from](#)  
236 the Kargin interstadial. Deposits from the L14-02 core from the Yedoma hill yielded radiocarbon ages  
237 between 33.1–62.8 ka BP, which corresponds to deposition during the MIS3 Kargin interstadial.

238 Overall, the permafrost deposits showed a wide range in TOC contents [\(0.8–6.3 wt%\)](#), C/N [\(4.6–](#)  
239 [29.4\)](#), and  $\delta^{13}\text{C}_{\text{org}}$  [\(-29.0–22.8 ‰ VPDB\)](#), (Fig. 2). Generally higher TOC contents and C/N were found  
240 in deposits from the Holocene and Kargin interstadial than in deposits from the Sartan stadial (Mann-  
241 Whitney test,  $p < 0.017$ ), while the  $\delta^{13}\text{C}_{\text{org}}$ -values were significantly higher in Sartan stadial deposits  
242 (Mann-Whitney test,  $p < 0.001$ ).

243

## 244 4.2. [Greenhouse gas production potentials](#)

### 245 4.2.1. Muostakh Island

246 Based on the TOC content, CO<sub>2</sub> production after 134 incubation days from sediment samples from the  
247 MUO12 sequence ranged between 4.8–60.7 mg CO<sub>2</sub>-C g<sup>-1</sup> OC under aerobic conditions and 0.5–20.9  
248 mg CO<sub>2</sub>-C g<sup>-1</sup> OC under anaerobic conditions (Fig. 3). Higher aerobic CO<sub>2</sub> production was generally  
249 observed in the lowermost Kargin deposits between 11.3–15.6 mbs ([Table 2](#)) but elevated CO<sub>2</sub>  
250 production ~~rates werewas~~ also observed at 1.6 mbs, 6 mbs, and 10 mbs. Under anaerobic conditions,  
251 the highest production was observed at 6 mbs (~~19.3 ± 1.4 mg CO<sub>2</sub>-C g<sup>-1</sup> OC~~), which was nearly twice as  
252 high as in most other samples. No methanogenesis was observed in any Muostakh Island samples over  
253 the 134-day incubation period.

254

### 255 4.2.2. Buor Khaya Peninsula

256 After 134 incubation days, CO<sub>2</sub> production in BK8 core samples ranged between 2.2–64.1 mg CO<sub>2</sub>-C g<sup>-1</sup>  
257 OC aerobically and 2.2–17.1 mg CO<sub>2</sub>-C g<sup>-1</sup> OC anaerobically (Fig. 4), which is within the same range as  
258 production in samples from Muostakh Island over the same incubation period ([Table 2](#)). The highest  
259 production was observed in the active layer. Production then decreased sharply between 0.5–3.2 mbs  
260 but increased again in Kargin interstadial deposits below the ice-wedge. Methanogenesis was only  
261 observed in the active layer, but in much smaller quantity than anaerobic CO<sub>2</sub> ~~production (0.37 ± 0.22~~  
262 ~~mg CH<sub>4</sub>-C g<sup>-1</sup> OC compared to 13.3 ± 3.6 mg CO<sub>2</sub>-C g<sup>-1</sup> OC).~~

263 To assess the ~~long-term decomposability of OC over longer periods~~, all BK8 core samples were  
264 incubated for a total of 785 days. After 785 incubation days, CO<sub>2</sub> production ranged between 4.6–131.1  
265 mg CO<sub>2</sub>-C g<sup>-1</sup> OC under aerobic conditions and 2.2–43.0 mg CO<sub>2</sub>-C g<sup>-1</sup> OC under anaerobic conditions.  
266 CO<sub>2</sub> production rates, however, decreased sharply within the first weeks of incubation. On average, 58  
267 ± 12% of the aerobically and 86 ± 24% of the anaerobically produced CO<sub>2</sub> after 785 incubation days was  
268 already produced within the first 134 days. In contrast, CH<sub>4</sub> production in the active layer increased 30-  
269 fold ~~between 134 and 785 incubation days to 11.4 ± 3.0 mg CH<sub>4</sub>-C g<sup>-1</sup> OC~~. Additionally, two out of three  
270 replicates at 10 mbs also showed active methanogenesis ~~between 134 and after 785 days. The total~~  
271 ~~CH<sub>4</sub> production after 785 days accounted for 17 and 50% of the total carbon production in those samples,~~  
272 ~~respectively (4.0 mg CH<sub>4</sub>-C g<sup>-1</sup> OC and 12.7 mg CH<sub>4</sub>-C g<sup>-1</sup> OC, respectively).~~

273

### 274 4.2.3. Bol'shoy Lyakhovsky Island

275 Aerobic CO<sub>2</sub> production after 134 incubation days in samples from the L14 cores ranged between 3.7–  
276 18.9 mg CO<sub>2</sub>-C g<sup>-1</sup> OC (Fig. 5). The mean aerobic CO<sub>2</sub> production in all MIS 3 Kargin interstadial deposits  
277 from Bol'shoy Lyakhovsky Island (~~9.2 ± 4.7 mg CO<sub>2</sub>-C g<sup>-1</sup> OC~~) was significantly lower (Mann-Whitney  
278 test, p < 0.001) than CO<sub>2</sub> production in MIS 3 deposits from Muostakh Island (~~32.2 ± 15.6 mg CO<sub>2</sub>-C g<sup>-1</sup>~~  
279 ~~OC~~) and the Buor Khaya Peninsula (Table 2, ~~26.0 ± 12.6 mg CO<sub>2</sub>-C g<sup>-1</sup> OC~~). Anaerobic CO<sub>2</sub> production  
280 in Kargin deposits from Bol'shoy Lyakhovsky Island ranged between 3.2–11.6 mg CO<sub>2</sub>-C g<sup>-1</sup> OC, which  
281 was within the same range as production observed from the other two locations. No CH<sub>4</sub> production was  
282 observed in any L14 samples after 134 days.

283 After 785 incubation days, aerobic and anaerobic CO<sub>2</sub> production ranged between 11.0–55.2 mg  
284 CO<sub>2</sub>-C g<sup>-1</sup> OC and 3.0–27.0 mg CO<sub>2</sub>-C g<sup>-1</sup> OC, respectively. Active methanogenesis was only observed  
285 in two out of three replicates from the active layer from the L14-05 core. However, (~~0.41 mg CH<sub>4</sub>-C g<sup>-1</sup>~~  
286 ~~OC and 0.63 mg CH<sub>4</sub>-C g<sup>-1</sup> OC~~). CH<sub>4</sub> production was ~~therefore~~ an order of magnitude lower than  
287 anaerobic CO<sub>2</sub> production in the same sample (~~5.7 mg CO<sub>2</sub>-C g<sup>-1</sup> OC and 4.6 mg CO<sub>2</sub>-C g<sup>-1</sup> OC~~) and  
288 also an order of magnitude smaller than CH<sub>4</sub> production in the active layer from the Buor Khaya  
289 Peninsula.

290

### 291 4.3. Decomposability of permafrost OM deposited under different climatic regimes

292 Overall, permafrost OM deposited during the MIS 3 Kargin interstadial supported the highest greenhouse  
293 gas production (Fig. 6). After 134 days of aerobic incubation, 0.2–6.1% of the initially available OC (~~mean~~  
294 ~~2.3 ± 1.4%~~) was decomposed to CO<sub>2</sub>. This was significantly more (Mann-Whitney test, p < 0.001) than  
295 in deposits from the Holocene and late glacial transition, where production ranged between 0.4–4.0%  
296 (~~mean 1.2 ± 0.8%~~). The aerobic CO<sub>2</sub> production in MIS 2 Sartan stadial deposits ranged between 0.5–  
297 4.2% (~~mean 1.7 ± 1.2 %~~). Anaerobically, 3.3 times less CO<sub>2</sub> was produced (Pearson correlation  
298 coefficient r = 0.63, p < 0.001). The lowest production was observed in Holocene and late glacial  
299 transition deposits, where 0.1–1.1 % of the OC was anaerobically decomposed to CO<sub>2</sub> (~~mean 0.5 ± 0.3~~).  
300 This was significantly less (Mann-Whitney test, p < 0.01) than in Yedoma glacial deposits, where 0.4–  
301 2.1% (~~mean 0.9 ± 0.5%~~) and 0.2–1.6 % of initial OC (~~mean 0.7 ± 0.3%~~) were decomposed in Sartan  
302 stadial and Kargin interstadial deposits, respectively.

303

## 304 5 Discussion

### 305 5.1. Organic matter decomposability

306 The ice-rich permafrost deposits of Muostakh Island, the Buor Khaya Peninsula, and Bol'shoy  
307 Lyakhovsky Island are typical for northeast Siberia and the geochemical OM characteristics (TOC, C/N,  
308  $\delta^{13}\text{C}_{\text{org}}$ ) were all within the range of other permafrost deposits in the region (Schirrneister et al., 2011).

309 However, a better understanding of the differences in OM decomposability is needed to estimate the  
310 future contribution of thawing permafrost landscapes to future greenhouse gas fluxes. ~~We hypothesized,~~  
311 ~~that the climatic conditions during deposition affected the amount and decomposability of preserved OM~~  
312 ~~and thus greenhouse gas production potentials after thaw. OM decomposability in degrading ice-rich~~  
313 ~~permafrost therefore needs to be interpreted against the paleo-environmental background.~~

314 The highest CO<sub>2</sub> production potentials from permafrost samples in the BK8 core were observed below  
315 the ice wedge between 8.35–16 mbs (Fig. 3). For this core section, which was deposited during the MIS  
316 3 Kargin interstadial (Schirrneister et al., 2017), (Zimmermann et al., (2017b) report a high taxonomic  
317 richness of vascular plants with high proportions of swamp and aquatic taxa, pointing towards a water-  
318 saturated environment at the time of deposition, likely a low-centered ice-wedge polygon. Furthermore,  
319 ~~(Stapel et al., (2016) report high concentrations of branched glycerol dialkyl glycerol tetraether (br-~~  
320 ~~GDGT), a microbial membrane compound, at 10 mbs, 11.2 mbs, and 15 mbs, indicative of a soil microbial~~  
321 ~~community, which developed when the climate was relatively warm and wet. Together with higher TOC~~  
322 ~~contents at these depths, this suggests accumulation of relatively undecomposed OM under anaerobic~~  
323 ~~conditions, which can be quickly decomposed after thaw (de Klerk et al., 2011), resulting in higher CO<sub>2</sub>~~  
324 ~~production.~~ One way to analyze the OM source in more detail is sedimentary ancient DNA (sedaDNA),  
325 ~~which can be used to reconstruct local plant communities and infer predominant climatic conditions~~  
326 ~~(Willerslev et al., 2004). In the BK8 core, a total of 134 vascular plants and 20 bryophytes were identified~~  
327 ~~(Zimmermann et al., 2017b). *Salix*, Poaceae and Cyperaceae, whose roots are a main OM source in~~  
328 ~~tundra soils (Iversen et al., 2015), are present throughout the core. The taxonomic richness was highest~~  
329 ~~between 8.35–16 mbs, where also high CO<sub>2</sub> production was observed. This core section, which belongs~~  
330 ~~to the MIS 3 Kargin interstadial (Schirrneister et al., 2017), was dominated by swamp and aquatic taxa,~~  
331 ~~pointing towards a water-saturated environment, likely a low-centered ice-wedge polygon (Zimmermann~~  
332 ~~et al., 2017b). Together with higher TOC contents at these depths, this suggests accumulation of~~  
333 ~~relatively undecomposed OM under anaerobic conditions, which can be quickly decomposed after thaw~~  
334 ~~(de Klerk et al., 2011). Furthermore, high concentrations of branched glycerol dialkyl glycerol tetraether~~

335 ~~(br-GDGT), a microbial membrane compound, are indicative of a soil microbial community, which~~  
336 ~~developed when the climate was relatively warm and wet (Stapel et al., 2016). Overall, br-GDGT~~  
337 ~~concentrations were highest at 10 mbs, 11.2 mbs, and 15 mbs (Stapel et al., 2016), which corresponds~~  
338 ~~to the same levels where the highest CO<sub>2</sub> production was observed.~~ In contrast, lower abundance of  
339 swamp taxa and higher abundance of terrestrial taxa at 8.8 mbs and ~~>~~below 15 mbs (Zimmermann et  
340 al., 2017b), suggest that intermittently drier conditions existed. This resulted in accelerated OM  
341 decomposition under aerobic conditions prior to OM incorporation into the permafrost and therefore lower  
342 TOC contents as well as lower CO<sub>2</sub> production potentials at these depths as overserved in this study.

343 Sediments above the ice-wedge in the BK8 core showed similar TOC contents, C/N, and  $\delta^{13}\text{C}_{\text{org}}$ -  
344 values compared to the rest of the core, but CO<sub>2</sub> production was consistently low in this section. This ~3  
345 m long core section yielded radiocarbon ages of 11.4–10.1 ka BP (Schirrmeister et al., 2017), which  
346 corresponds to the late glacial-early Holocene transition. After the Last Glacial Maximum (LGM),  
347 temperatures were favorable for increased microbial decomposition of active layer OM, which led to the  
348 preservation of comparatively stable OM fractions after the material was incorporated into the  
349 permafrost. ~~Similar conclusions can be drawn for Holocene deposits in thermokarst landforms or on top~~  
350 ~~of Yedoma deposits. On the one hand, they received fresh OM inputs, which explains their relatively high~~  
351 ~~TOC contents (Strauss et al., 2015). On the other hand, intensive thermokarst development during the~~  
352 ~~late glacial transition and the early Holocene likely resulted in higher decomposition rates in thawed soils~~  
353 ~~and the loss of labile OM compounds before the sediments were refrozen when climate conditions~~  
354 ~~deteriorated after the Holocene climate optimum.~~ If these sediments were to thaw again in the future,  
355 results from the current study suggest that the decomposability of the remaining OM will be comparatively  
356 low. However, deeper rooting, cryoturbation, and post-thaw leaching of labile OM from vegetation could  
357 stimulate the decomposition and greenhouse gas production from the more stable OM through positive  
358 priming (Fontaine et al., 2007). Both the chemical structure (Di Lonardo et al., 2017) and the frequency  
359 of labile ~~organic matter~~OM inputs (Fan et al., 2013) influence the size of the priming effect. For permafrost  
360 soils, it has also been shown, that the priming effect is larger at lower temperatures (Walz et al., 2017).  
361 ~~Although Thus,~~ climatic conditions influence the vegetation composition and OM source on a regional  
362 level, but the local depositional environment as well as post-depositional processes likely also control  
363 the amount and decomposability of the OM that is presently incorporated into permafrost.

364 First results of *in situ* CO<sub>2</sub> fluxes from Muostakh Island were published by Vonk et al. (2012). Based  
365 on the downslope decrease in OC contents, ~~T~~they estimate that 66% of the thawed-out Yedoma OC

366 ~~from degrading ice-rich permafrost deposits~~ can be decomposed to ~~greenhouse gases~~CO<sub>2</sub> and released  
367 back to the atmosphere before the material is reburied in the Laptev Sea. This is an order of magnitude  
368 more than what the results from current incubation study suggest, where after 134 days only 0.4–6.0%  
369 of the Yedoma OC from Muostakh Island were aerobically decomposed to CO<sub>2</sub>. However, ~~n~~No further  
370 detailed palynological or microbial biomarker studies are yet available for the MUO12 sequence. The  
371 closest reference locations is the comprehensive permafrost record at the Mamontovy Khayata section  
372 on the Bykovsky Peninsula (Andreev et al., 2002; Sher et al., 2005). Between 58– and 12 ka BP  
373 (Schirrneister et al., 2002b), fine-grained material accumulated on the large flat foreland plain of the  
374 today Bykovsky Peninsula area that was exposed at a time of lower sea level (Grosse et al., 2007). Sea  
375 level rise after the last glacial period, coastal erosion, and marine ingression of thermokarst basins  
376 formed the Buor Khaya Bay and eventually separated Muostakh Island from the Bykovsky Peninsula  
377 (Grosse et al., 2007; Romanovskii et al., 2004). ~~Today, the distance between the northern tip of Muostakh~~  
378 ~~Island and the southern tip of the Bykovsky Peninsula is about 16 km. Between 58–12 ka BP~~  
379 ~~(Schirrneister et al., 2002), fine-grained material accumulated on the large flat foreland plain of the today~~  
380 ~~Bykovsky Peninsula area that was exposed at a time of lower sea level (Grosse et al., 2007). The~~  
381 ~~distance between Muostakh Island and the Buor Khaya Peninsula is about 80 km.~~ It is ~~therefore~~ likely  
382 that the deposition regimes on Muostakh Island and the Buor Khaya Peninsula were similar to the regime  
383 at the Bykovsky Peninsula. This conclusion is also supported by similar OM decomposability. After 134  
384 incubation days, the amount of aerobic and anaerobic CO<sub>2</sub> production did not differ significantly (Mann-  
385 Whitney test, p = 0.339) between MIS 3 Kargin deposits from Muostakh Island (~~3.2 ± 1.6% of initial OC~~  
386 ~~aerobically and 0.7 ± 0.6% anaerobically~~) and the BK8 core Buor Khaya Peninsula (Table 22.7 ± 1.2%  
387 aerobically and 0.8 ± 0.3 % anaerobically), which suggests that the deposits formed under similar  
388 conditions. In contrast, Under aerobic conditions, CO<sub>2</sub> production ~~of in~~ MIS 3 deposits from Bol'shoy  
389 Lyakhovsky Island in the eastern Laptev Sea was nearly three times lower (~~0.9 ± 0.5% of the initial OC~~  
390 ~~after 134 days~~) than observed for Muostakh Island and the Buor Khaya Peninsula in the central Laptev  
391 Sea. Considerably lower temperatures and precipitation characterize the modern-current climate on  
392 Bol'shoy Lyakhovsky Island. It is also likely that regional differences between the eastern and central  
393 Laptev Sea region would have affected the paleo-climate (Anderson and Lozhkin, 2001; Lozhkin and  
394 Anderson, 2011; Wetterich et al., 2011, 2014). Different summer temperatures, precipitation, thaw depth,  
395 and vegetation composition could explain regional differences in OM quantity and decomposability.  
396 Interestingly, the differences in the amount of OC that was aerobically decomposed were mostly due to

397 ~~differences in the initial CO<sub>2</sub> production rates. Maximum CO<sub>2</sub> production rates during the first weeks of~~  
398 ~~incubation of Muostakh Island and Buor Khaya deposits were up to four times higher than in deposits~~  
399 ~~from Bol'shoy Lyakhovsky Island. However, long-term production rates after >130 incubation days did~~  
400 ~~no longer differ considerably between the different locations (median 23.3 μg CO<sub>2</sub>-C g<sup>-1</sup> OC d<sup>-1</sup>). These~~  
401 ~~rates are within the range of other long-term production rates from Yedoma deposits in northeast Siberia~~  
402 ~~(Dutta et al., 2006; Knoblauch et al., 2013) and Alaska (Lee et al., 2012). Considering the large slowly~~  
403 ~~decomposing permafrost OC pool (Schädel et al., 2014), long-term decomposition rates are likely to~~  
404 ~~provide more reliable projections of future greenhouse gas emissions from degrading permafrost~~  
405 ~~landscapes.~~

406 A distinctive feature of the Muostakh Island sequence is the preservation of MIS 2 Sartan deposits,  
407 which are only sparsely preserved in northeast Siberia (Wetterich et al., 2011). Interestingly, mean  
408 aerobic CO<sub>2</sub> production in Sartan deposits from Muostakh Island was lower than in Kargin deposits, but  
409 slightly higher under anaerobic conditions, but the difference was not statistically significant (Mann-  
410 Whitney test, p = 0.205). The rapid deposition of 8 m thick comparatively coarse-grained material in just  
411 a few thousand years between 20 and –16 ka BP were unfavorable for the development of a stable land  
412 surface and the establishment of a vegetation cover comparable to the Kargin interstadial or Holocene  
413 periods (Meyer et al., unpublished data). Pollen analysis from the corresponding sections on the  
414 Bykovsky Peninsula (Andreev et al., 2002) and Kurungnakh Island in the Lena River Delta (Schirrmeister  
415 et al., 2008; Wetterich et al., 2008) suggest relatively cold and dry summer conditions during this stadial  
416 with sparse vegetation. Relatively undecomposed OM was quickly buried, before it could be transformed  
417 to greenhouse gases.

## 418

### 419 **5.2. Long-term production potentialsMulti-annual incubation**

420 The 785-day incubation of permafrost samples from the Buor Khaya Peninsula and Bol'shoy  
421 Lyakhovsky Island revealed Long-term greenhouse gas production measurements after 785 days  
422 showed that 51% of the aerobically and 83% of the anaerobically produced CO<sub>2</sub> were already produced  
423 within the first 134 incubation days, highlighting the non-linearity of OM decomposition dynamics  
424 (Knoblauch et al., 2013; Schädel et al., 2014) and the importance of the labile OC pool in short term  
425 incubations. Maximum CO<sub>2</sub> production rates were generally reached within the first 100 incubation days.  
426 After the initial peak, CO<sub>2</sub> production rates remained consistently low (median 23.3 μg CO<sub>2</sub>-C g<sup>-1</sup> OC d<sup>-1</sup>  
427 aerobically and 3.2 μg CO<sub>2</sub>-C g<sup>-1</sup> OC d<sup>-1</sup> anaerobically). These rates are within the range of other multi-

428 annual production rates from Yedoma deposits in northeast Siberia (Dutta et al., 2006; Knoblauch et al.,  
429 2013) and Alaska (Lee et al., 2012).

430 Assuming no new input of labile OM (e.g. from ~~modern~~ the current vegetation), decomposition rates  
431 are likely to remain low after the labile pool is depleted. Short-term greenhouse gas production and  
432 release from thawing ice-rich permafrost will therefore mainly depend on the size of the labile pool. A  
433 synthesis study of several incubations studies from high-latitude soils, including Yedoma deposits,  
434 estimated the size of the labile OC pool to be generally less than <5% of the TOC (Schädel et al., 2014).  
435 For Yedoma deposits on nearby Kurungnakh Island in the Lena River delta, Knoblauch et al. (2013)  
436 estimated the size of the labile pool to be even smaller (less than <2%). -Considering the large slowly  
437 decomposing permafrost OC pool (Schädel et al., 2014), long-term decomposition rates are therefore  
438 likely to provide more reliable projections of future greenhouse gas emissions from production in  
439 degrading permafrost landscapes.

440

441

### 442 **5.3. Methanogenesis**

443 CH<sub>4</sub> production from Yedoma deposits, or the lack thereof, is a highly controversial topic in permafrost  
444 research (Knoblauch et al., 2018; Rivkina et al., 1998; Treat et al., 2015). In the current work, active  
445 methanogenesis was only observed in ~~the active layer and 2~~ two out of 38 Yedoma samples from the  
446 BK8 core, ~~but only after a long lag phase. Within 134 incubation days, no samples from Muostakh~~  
447 ~~Island produced any CH<sub>4</sub>.~~ In those samples showing active methanogenesis, CH<sub>4</sub> production continued  
448 to rise over the 785 incubation days, which is in contrast to anaerobic CO<sub>2</sub> production, which decreased  
449 with increasing incubation time. Rising CH<sub>4</sub> production rates indicate that methanogenic communities  
450 still grow in these samples and were not limited by substrate supply. Chemical pore water and bulk  
451 sediment analyses from the BK8 core showed that there are high concentrations of both free and OM-  
452 bound acetate present in Yedoma deposits, indicating a high substrate potential for methanogenesis  
453 (Stapel et al., 2016). Knoblauch et al. (2018) showed that the small contribution of methanogenesis to  
454 overall anaerobic permafrost OM decomposition found in short-term incubation studies (Treat et al.,  
455 2015) is due to the absence of an active methanogenic community. On a multi-annual timescale,  
456 methanogenic communities become active and equal amounts of CO<sub>2</sub> and CH<sub>4</sub> are produced from  
457 permafrost OM under anaerobic conditions. Under future climate warming and renewed thermokarst  
458 activity, high levels of CH<sub>4</sub> production can locally be expected, but depend on favorable conditions such

459 as above-zero temperatures and anaerobic conditions. It can be expected that the development of an  
460 active methanogenic community, e.g. by growth or downward migration of modern methanogenic  
461 organisms, will lead to elevated long-term CH<sub>4</sub> production in these deposits (Knoblauch et al., 2018).

462

## 463 **6 Conclusion**

464 In this study, we investigated greenhouse gas production potentials in degrading ice-rich permafrost  
465 deposits from three locations in northeast Siberia. We hypothesized, that the climatic conditions during  
466 deposition affected the amount and decomposability of preserved OM and thus greenhouse gas  
467 production potentials after thaw. OM decomposability in degrading ice-rich permafrost therefore needs  
468 to be interpreted against the paleo-environmental background. It could be shown that Yedoma deposits  
469 generally contained more labile OM than Holocene deposits. However, in addition to the regional climate  
470 conditions at the time of OM deposition, local depositional environments also influenced the amount and  
471 decomposability of the preserved fossil OM. Within the deposits of the MIS 3 Kargin interstadial,  
472 sediments deposited under wet and possibly anaerobic conditions produced more CO<sub>2</sub> than sediments  
473 deposited under drier aerobic conditions. Further, deposits from the central Laptev Sea region produced  
474 2–3 times more CO<sub>2</sub> than deposits from the eastern Laptev Sea region. It is therefore likely, that OM  
475 decomposability of the vast Yedoma landscape cannot be generalized solely based on the stratigraphic  
476 position. Furthermore, it is expected that CH<sub>4</sub> production will play a more prominent role after active  
477 methanogenic communities have established since abundant substrates for methanogenesis were  
478 present.

479

## 480 **Data availability**

481 All shown data sets as well as the temporal evolution of CO<sub>2</sub> and CH<sub>4</sub> production over the whole  
482 incubation period is available at <https://doi.pangaea.de/10.1594/PANGAEA.892950> (Walz et al.,  
483 2018). <https://www.pangaea.de/> (follows after acceptance and includes all shown datasets)

484

## 485 **Author contributions**

486 JW and CK designed the study. TO collected sediment samples on Muostakh Island and LS collected  
487 cores from the Buor Khaya Peninsula and Bol'shoy Lyakhovsky Island. JW and RT performed the  
488 laboratory analyses, with guidance from CK and EMP. JW performed data analyses and wrote the  
489 manuscript with contributions from all authors.

491 **Acknowledgements**

492 This research was supported by the German Ministry of Education and Research as part of [the](#) projects  
 493 CarboPerm (grant no. 03G0836A, 03G0836B) and KoPf (grant no. 03F0764A). We [further](#) acknowledge  
 494 the financial support through the German Research Foundation (DFG) to EMP and CK through the  
 495 Cluster of Excellence “CliSAP” (EXC177), University Hamburg and to TO (grant OP 217/3-1). We also  
 496 thank the Russian and German participants of the drilling and sampling expeditions, especially Mikhail  
 497 N. Grigoriev (Melnikov Permafrost Institute, Yakutsk), Hanno Meyer and Pier Paul Overduin (both Alfred-  
 498 Wegener-Institute, Potsdam). Additional thanks go to Georg Schwamborn (Alfred-Wegener-Institute,  
 499 Potsdam) for his assistance with core subsampling and Birgit Schwinge (Institute of Soil Science,  
 500 Hamburg) for her help in the laboratory. [We are also immensely grateful for the two anonymous reviews](#)  
 501 [on a previous version of this manuscript.](#)

502

503 **References**

- 504 Anderson, P. M. and Lozhkin, A. V.: The Stage 3 interstadial complex (Karginiskii/middle Wisconsinan  
 505 interval) of Beringia: variations in paleoenvironments and implications for paleoclimatic interpretations,  
 506 *Quat. Sci. Rev.*, 20(1–3), 93–125, doi:10.1016/S0277-3791(00)00129-3, 2001.
- 507 Andreev, A. A., Schirrmeister, L., Siegert, C., Bobrov, A. A., Demske, D., Seiffert, M. and Hubberten, H.-  
 508 W.: Paleoenvironmental changes in northeastern Siberia during the Late Quaternary - Evidence from  
 509 pollen records of the Bykovsky Peninsula, *Polarforschung*, 70, 13–25, 2002.
- 510 Andreev, A. A., Grosse, G., Schirrmeister, L., Kuznetsova, T. V., Kuzmina, S. A., Bobrov, A. A., Tarasov,  
 511 P. E., Novenko, E. Y., Meyer, H., Derevyagin, A. Y., Kienast, F., Bryantseva, A. and Kunitsky, V. V.:  
 512 Weichselian and Holocene palaeoenvironmental history of the Bol'shoy Lyakhovsky Island, New  
 513 Siberian Archipelago, Arctic Siberia, *Boreas*, 38(1), 72–110, doi:10.1111/j.1502-3885.2008.00039.x,  
 514 2009.
- 515 Andreev, A. A., Schirrmeister, L., Tarasov, P. E., Ganopolski, A., Brovkin, V., Siegert, C., Wetterich, S.  
 516 and Hubberten, H.-W.: Vegetation and climate history in the Laptev Sea region (Arctic Siberia) during  
 517 Late Quaternary inferred from pollen records, *Quat. Sci. Rev.*, 30(17–18), 2182–2199,  
 518 doi:10.1016/j.quascirev.2010.12.026, 2011.
- 519 Brown, J., Ferrians Jr, O. J., Heginbottom, J. A. and Melnikov, E. S.: Circum-Arctic map of permafrost  
 520 and ground-ice conditions. Boulder, CO: National Snow and Ice Data Center/World Data Center for  
 521 Glaciology, Digit. media, 1998.
- 522 Bulygina, O. N. and Razuvaev, V. N.: Daily temperature and precipitation data for 518 Russian  
 523 meteorological stations, Carbon Dioxide Information Analysis Center, Oak Ridge National Laboratory,  
 524 U.S. Department of Energy, Oak Ridge, Tennessee (USA)., 2012.

- 525 Carroll, J. J., Slupsky, J. D. and Mather, A. E.: The solubility of carbon dioxide in water at low pressure,  
526 J. Phys. Chem. Ref. Data, 20(6), 1201, doi:10.1063/1.555900, 1991.
- 527 CAVM Team: Circumpolar Arctic Vegetation Map (1:7,500,000 scale), Conservation of Arctic Flora and  
528 Fauna (CAFF) Map No. 1, U.S. Fish and Wildlife Service, Anchorage, Alaska., 2003.
- 529 Drozdov, D. S., Rivkin, F. M., Rachold, V., Ananjeva-Malkova, G. V., Ivanova, N. V., Chehina, I. V.,  
530 Koreisha, M. M., Korostelev, Y. V. and Melnikov, E. S.: Electronic atlas of the Russian Arctic coastal  
531 zone, Geo-Marine Lett., 25(2–3), 81–88, doi:10.1007/s00367-004-0189-7, 2005.
- 532 Dutta, K., Schuur, E. A. G., Neff, J. C. and Zimov, S. A.: Potential carbon release from permafrost soils  
533 of Northeastern Siberia, Glob. Chang. Biol., 12(12), 2336–2351, doi:10.1111/j.1365-2486.2006.01259.x,  
534 2006.
- 535 van Everdingen, R.: Multi-language glossary of permafrost and related ground-ice terms, [online]  
536 Available from: <http://nsidc.org/fgdc/glossary/> (Accessed 1 January 2015), 2005.
- 537 Fan, Z., Jastrow, J. D., Liang, C., Matamala, R. and Miller, R. M.: Priming effects in boreal black spruce  
538 forest soils: Quantitative evaluation and sensitivity analysis, PLoS One, 8(10), e77880,  
539 doi:10.1371/journal.pone.0077880, 2013.
- 540 Fontaine, S., Barot, S., Barré, P., Bdioui, N., Mary, B. and Rumpel, C.: Stability of organic carbon in deep  
541 soil layers controlled by fresh carbon supply, Nature, 450(7167), 277–280, doi:10.1038/nature06275,  
542 2007.
- 543 Grigoriev, M. N., Overduin, P. P., Schirrmeister, L. and Wetterich, S.: Scientific permafrost drilling  
544 campaign, in Russian-German cooperation SYSTEM LAPTEV SEA: The Expeditions Laptev Sea -  
545 Mamontov Klyk 2011 & Buor Khaya 2012, vol. 664, edited by F. Günther, P. P. Overduin, A. S. Makarov,  
546 and M. N. Grigoriev, pp. 75–86, Reports on Polar and Marine Research, 2013.
- 547 Grosse, G., Schirrmeister, L., Siegert, C., Kunitsky, V. V., Slagoda, E. A., Andreev, A. A. and Dereviagyn,  
548 A. Y.: Geological and geomorphological evolution of a sedimentary periglacial landscape in Northeast  
549 Siberia during the Late Quaternary, Geomorphology, 86(1–2), 25–51,  
550 doi:10.1016/j.geomorph.2006.08.005, 2007.
- 551 Grosse, G., Robinson, J. E., Bryant, R., Taylor, M. D., Harper, W., DeMasi, A., Kyker-Snowman, E.,  
552 Veremeeva, A., Schirrmeister, L. and Harden, J.: Distribution of late Pleistocene ice-rich syngenetic  
553 permafrost of the Yedoma Suite in east and central Siberia, Russia, Geol. Surv. Open File Rep. 1078,  
554 1–37 [online] Available from: <http://epic.awi.de/33878/>, 2013.
- 555 Günther, F., Overduin, P. P., Sandakov, a. V., Grosse, G. and Grigoriev, M. N.: Short- and long-term  
556 thermo-erosion of ice-rich permafrost coasts in the Laptev Sea region, Biogeosciences, 10(6), 4297–  
557 4318, doi:10.5194/bg-10-4297-2013, 2013.
- 558 Günther, F., Overduin, P. P., Yakshina, I. A., Opel, T., Baranskaya, A. V. and Grigoriev, M. N.: Observing  
559 Muostakh disappear: Permafrost thaw subsidence and erosion of a ground-ice-rich island in response  
560 to arctic summer warming and sea ice reduction, Cryosph., 9(1), 151–178, doi:10.5194/tc-9-151-2015,  
561 2015.
- 562 Harden, J. W., Koven, C. D., Ping, C.-L., Hugelius, G., David McGuire, A., Camill, P., Jorgenson, T.,  
563 Kuhry, P., Michaelson, G. J., O'Donnell, J. A., Schuur, E. A. G., Tarnocai, C., Johnson, K. and Grosse,  
564 G.: Field information links permafrost carbon to physical vulnerabilities of thawing, Geophys. Res. Lett.,

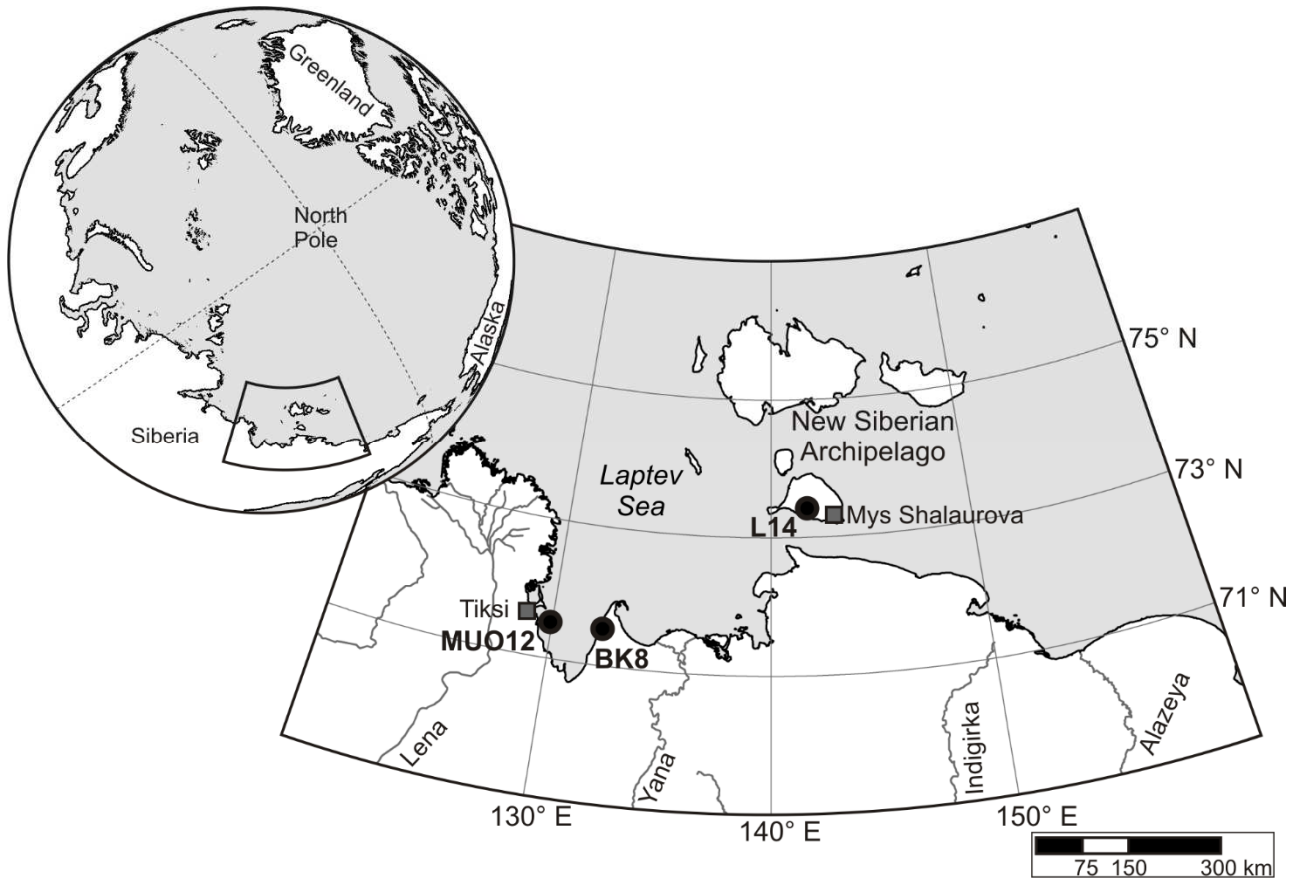
- 565 39(15), 1–6, doi:10.1029/2012GL051958, 2012.
- 566 Hugelius, G., Routh, J., Kuhry, P. and Crill, P.: Mapping the degree of decomposition and thaw  
567 remobilization potential of soil organic matter in discontinuous permafrost terrain, *J. Geophys. Res.*  
568 *Biogeosciences*, 117(G2), G02030, doi:10.1029/2011JG001873, 2012.
- 569 Hugelius, G., Strauss, J., Zubrzycki, S., Harden, J. W., Schuur, E. A. G., Ping, C.-L., Schirrmeister, L.,  
570 Grosse, G., Michaelson, G. J., Koven, C. D., O'Donnell, J. A., Elberling, B., Mishra, U., Camill, P., Yu,  
571 Z., Palmtag, J. and Kuhry, P.: Estimated stocks of circumpolar permafrost carbon with quantified  
572 uncertainty ranges and identified data gaps, *Biogeosciences*, 11(23), 6573–6593, doi:10.5194/bg-11-  
573 6573-2014, 2014.
- 574 Iversen, C. M., Sloan, V. L., Sullivan, P. F., Euskirchen, E. S., McGuire, A. D., Norby, R. J., Walker, A.  
575 P., Warren, J. M. and Wulfschleger, S. D.: The unseen iceberg: Plant roots in arctic tundra, *New Phytol.*,  
576 205(1), 34–58, doi:10.1111/nph.13003, 2015.
- 577 Kanevskiy, M., Shur, Y., Fortier, D., Jorgenson, M. T. and Stephani, E.: Cryostratigraphy of late  
578 Pleistocene syngenetic permafrost (yedoma) in northern Alaska, Itkillik River exposure, *Quat. Res.*,  
579 75(3), 584–596, doi:10.1016/j.yqres.2010.12.003, 2011.
- 580 de Klerk, P., Donner, N., Karpov, N. S., Minke, M. and Joosten, H.: Short-term dynamics of a low-centred  
581 ice-wedge polygon near Chokurdakh (NE Yakutia, NE Siberia) and climate change during the last ca  
582 1250 years, *Quat. Sci. Rev.*, 30(21–22), 3013–3031, doi:10.1016/j.quascirev.2011.06.016, 2011.
- 583 Knoblauch, C., Beer, C., Sosnin, A., Wagner, D. and Pfeiffer, E.-M.: Predicting long-term carbon  
584 mineralization and trace gas production from thawing permafrost of Northeast Siberia, *Glob. Chang.*  
585 *Biol.*, 19(4), 1160–1172, doi:10.1111/gcb.12116, 2013.
- 586 Knoblauch, C., Beer, C., Liebner, S., Grigoriev, M. N. and Pfeiffer, E.-M.: Methane production as key to  
587 the greenhouse gas budget of thawing permafrost, *Nat. Clim. Chang.*, 8(4), 309–312,  
588 doi:10.1038/s41558-018-0095-z, 2018.
- 589 Lee, H., Schuur, E. A. G., Inglett, K. S., Lavoie, M. and Chanton, J. P.: The rate of permafrost carbon  
590 release under aerobic and anaerobic conditions and its potential effects on climate, *Glob. Chang. Biol.*,  
591 18(2), 515–527, doi:10.1111/j.1365-2486.2011.02519.x, 2012.
- 592 Di Lonardo, D. P., De Boer, W., Klein Gunnewiek, P. J. A., Hannula, S. E. and Van der Wal, A.: Priming  
593 of soil organic matter: Chemical structure of added compounds is more important than the energy  
594 content, *Soil Biol. Biochem.*, 108, 41–54, doi:10.1016/j.soilbio.2017.01.017, 2017.
- 595 Lozhkin, A. V. and Anderson, P. M.: Forest or no forest: Implications of the vegetation record for climatic  
596 stability in Western Beringia during oxygen isotope stage 3, *Quat. Sci. Rev.*, 30(17–18), 2160–2181,  
597 doi:10.1016/j.quascirev.2010.12.022, 2011.
- 598 MacDougall, A. H. and Knutti, R.: Projecting the release of carbon from permafrost soils using a  
599 perturbed parameter ensemble modelling approach, *Biogeosciences*, 13(7), 2123–2136,  
600 doi:10.5194/bg-13-2123-2016, 2016.
- 601 Meyer, H., Opel, T. and Dereviagin, A.: Stratigraphic and sedimentological studies, in *Russian-German*  
602 *Cooperation SYSTEM LAPTEV SEA: The expedition Lena 2012*, pp. 79–82, Reports on Polar and  
603 *Marine Research*, 2015.
- 604 Millero, F., Huang, F., Graham, T. and Pierrot, D.: The dissociation of carbonic acid in NaCl solutions as

- 605 a function of concentration and temperature, *Geochim. Cosmochim. Acta*, 71(1), 46–55,  
606 doi:10.1016/j.gca.2006.08.041, 2007.
- 607 Morgenstern, A., Ulrich, M., Günther, F., Roessler, S., Fedorova, I. V., Rudaya, N. A., Wetterich, S.,  
608 Boike, J. and Schirrmeister, L.: Evolution of thermokarst in East Siberian ice-rich permafrost: A case  
609 study, *Geomorphology*, 201, 363–379, doi:10.1016/j.geomorph.2013.07.011, 2013.
- 610 Natali, S. M., Schuur, E. A. G., Mauritz, M., Schade, J. D., Celis, G., Crummer, K. G., Johnston, C.,  
611 Krapek, J., Pegoraro, E., Salmon, V. G. and Webb, E. E.: Permafrost thaw and soil moisture driving CO<sub>2</sub>  
612 and CH<sub>4</sub> release from upland tundra, *J. Geophys. Res. Biogeosciences*, 120(3), 525–537,  
613 doi:10.1002/2014JG002872, 2015.
- 614 Opel, T., Wetterich, S., Meyer, H., Dereviagin, A. Y., Fuchs, M. C. and Schirrmeister, L.: Ground-ice  
615 stable isotopes and cryostratigraphy reflect late Quaternary palaeoclimate in the Northeast Siberian  
616 Arctic (Oyogos Yar coast, Dmitry Laptev Strait), *Clim. Past*, 13(6), 587–611, doi:10.5194/cp-13-587-  
617 2017, 2017.
- 618 Overduin, P. P., Liebner, S., Knoblauch, C., Günther, F., Wetterich, S., Schirrmeister, L., Hubberten, H.-  
619 W. and Grigoriev, M. N.: Methane oxidation following submarine permafrost degradation: Measurements  
620 from a central Laptev Sea shelf borehole, *J. Geophys. Res. Biogeosciences*, 120, 1–14,  
621 doi:10.1002/2014JG002862.Received, 2015.
- 622 Ping, C. L., Jastrow, J. D., Jorgenson, M. T., Michaelson, G. J. and Shur, Y. L.: Permafrost soils and  
623 carbon cycling, *SOIL*, 1(1), 147–171, doi:10.5194/soil-1-147-2015, 2015.
- 624 Rivkina, E., Gilichinsky, D., Wagener, S., Tiedje, J. and McGrath, J.: Biogeochemical activity of anaerobic  
625 microorganisms from buried permafrost sediments, *Geomicrobiol. J.*, 15(3), 187–193,  
626 doi:10.1080/01490459809378075, 1998.
- 627 Romanovskii, N. N., Hubberten, H.-W., Gavrilov, A. V., Tumskoy, V. E. and Kholodov, A. L.: Permafrost  
628 of the east Siberian Arctic shelf and coastal lowlands, *Quat. Sci. Rev.*, 23(11–13), 1359–1369,  
629 doi:10.1016/j.quascirev.2003.12.014, 2004.
- 630 Schädel, C., Schuur, E. A. G., Bracho, R., Elberling, B., Knoblauch, C., Lee, H., Luo, Y., Shaver, G. R.  
631 and Turetsky, M. R.: Circumpolar assessment of permafrost C quality and its vulnerability over time using  
632 long-term incubation data, *Glob. Chang. Biol.*, 20(2), 641–652, doi:10.1111/gcb.12417, 2014.
- 633 Schirrmeister, L., Oezen, D. and Geyh, M. A.: <sup>230</sup>Th/U dating of frozen peat, Bol'shoy Lyakhovsky Island  
634 (Northern Siberia), *Quat. Res.*, 57(2), 253–258, doi:10.1006/qres.2001.2306, 2002a.
- 635 Schirrmeister, L., Siegert, C., Kuznetsova, T., Kuzmina, S., Andreev, A., Kienast, F., Meyer, H. and  
636 Bobrov, A.: Paleoenvironmental and paleoclimatic records from permafrost deposits in the Arctic region  
637 of Northern Siberia, *Quat. Int.*, 89(1), 97–118, doi:10.1016/S1040-6182(01)00083-0, 2002b.
- 638 Schirrmeister, L., Grosse, G., Kunitsky, V., Magens, D., Meyer, H., Dereviagin, A., Kuznetsova, T.,  
639 Andreev, A., Babiy, O., Kienast, F., Grigoriev, M., Overduin, P. P. and Preusser, F.: Periglacial landscape  
640 evolution and environmental changes of Arctic lowland areas for the last 60000 years (western Laptev  
641 Sea coast, Cape Mamontov Klyk), *Polar Res.*, 27(2), 249–272, doi:10.1111/j.1751-8369.2008.00067.x,  
642 2008.
- 643 Schirrmeister, L., Kunitsky, V., Grosse, G., Wetterich, S., Meyer, H., Schwamborn, G., Babiy, O.,  
644 Derevyagin, A. and Siegert, C.: Sedimentary characteristics and origin of the Late Pleistocene Ice

- 645 Complex on north-east Siberian Arctic coastal lowlands and islands – A review, *Quat. Int.*, 241(1–2), 3–  
646 25, doi:10.1016/j.quaint.2010.04.004, 2011.
- 647 Schirrmeister, L., Froese, D., Tumskoy, V., Grosse, G. and Wetterich, S.: Yedoma: Late Pleistocene ice-  
648 rich syngenetic permafrost of Beringia, in *Encyclopedia of Quaternary Science*, edited by S. A. Elias, pp.  
649 542–552, Elsevier, Amsterdam., 2013.
- 650 Schirrmeister, L., Schwamborn, G., Overduin, P. P., Strauss, J., Fuchs, M. C., Grigoriev, M., Yakshina,  
651 I., Rethemeyer, J., Dietze, E. and Wetterich, S.: Yedoma Ice Complex of the Buor Khaya Peninsula  
652 (southern Laptev Sea), *Biogeosciences*, 14(5), 1261–1283, doi:10.5194/bg-14-1261-2017, 2017.
- 653 Schneider von Deimling, T., Meinshausen, M., Levermann, A., Huber, V., Frieler, K., Lawrence, D. M.  
654 and Brovkin, V.: Estimating the near-surface permafrost-carbon feedback on global warming,  
655 *Biogeosciences*, 9(2), 649–665, doi:10.5194/bg-9-649-2012, 2012.
- 656 Schneider von Deimling, T., Grosse, G., Strauss, J., Schirrmeister, L., Morgenstern, A., Schaphoff, S.,  
657 Meinshausen, M. and Boike, J.: Observation-based modelling of permafrost carbon fluxes with  
658 accounting for deep carbon deposits and thermokarst activity, *Biogeosciences*, 12(11), 3469–3488,  
659 doi:10.5194/bg-12-3469-2015, 2015.
- 660 Schuur, E. A. G., McGuire, A. D., Schädel, C., Grosse, G., Harden, J. W., Hayes, D. J., Hugelius, G.,  
661 Koven, C. D., Kuhry, P., Lawrence, D. M., Natali, S. M., Olefeldt, D., Romanovsky, V. E., Schaefer, K.,  
662 Turetsky, M. R., Treat, C. C. and Vonk, J. E.: Climate change and the permafrost carbon feedback,  
663 *Nature*, 520(7546), 171–179, doi:10.1038/nature14338, 2015.
- 664 Schwamborn, G. and Schirrmeister, L.: Permafrost drilling on Bol'shoy Lyakhovsky, in *Russian-German  
665 Cooperation CARBOPERM: Field campaigns to Bol'shoy Lyakhovsky Island in 2014*, pp. 11–19., 2015.
- 666 Sher, A. V., Kuzmina, S. A., Kuznetsova, T. V. and Sulerzhitsky, L. D.: New insights into the Weichselian  
667 environment and climate of the East Siberian Arctic, derived from fossil insects, plants, and mammals,  
668 *Quat. Sci. Rev.*, 24(5–6), 533–569, doi:10.1016/j.quascirev.2004.09.007, 2005.
- 669 Shmelev, D., Veremeeva, A., Kraev, G., Kholodov, A., Spencer, R. G. M., Walker, W. S. and Rivkina, E.:  
670 Estimation and sensitivity of carbon storage in permafrost of north-eastern Yakutia, *Permafr. Periglac.  
671 Process.*, 28(2), 379–390, doi:10.1002/ppp.1933, 2017.
- 672 Stapel, J. G., Schirrmeister, L., Overduin, P. P., Wetterich, S., Strauss, J., Horsfield, B. and Mangelsdorf,  
673 K.: Microbial lipid signatures and substrate potential of organic matter in permafrost deposits:  
674 Implications for future greenhouse gas production, *J. Geophys. Res. Biogeosciences*, 121(10), 2652–  
675 2666, doi:10.1002/2016JG003483, 2016.
- 676 Stapel, J. G., Schwamborn, G., Schirrmeister, L., Horsfield, B. and Mangelsdorf, K.: Substrate potential  
677 of last interglacial to Holocene permafrost organic matter for future microbial greenhouse gas production,  
678 *Biogeosciences*, 15(7), 1969–1985, doi:10.5194/bg-15-1969-2018, 2018.
- 679 Strauss, J., Schirrmeister, L., Grosse, G., Wetterich, S., Ulrich, M., Herzsuh, U. and Hubberten, H.-  
680 W.: The deep permafrost carbon pool of the Yedoma region in Siberia and Alaska, *Geophys. Res. Lett.*,  
681 40(23), 6165–6170, doi:10.1002/2013GL058088, 2013.
- 682 Strauss, J., Schirrmeister, L., Mangelsdorf, K., Eichhorn, L., Wetterich, S. and Herzsuh, U.: Organic-  
683 matter quality of deep permafrost carbon – A study from Arctic Siberia, *Biogeosciences*, 12(7), 2227–  
684 2245, doi:10.5194/bg-12-2227-2015, 2015.

- 685 Strauss, J., Schirrmeister, L., Grosse, G., Fortier, D., Hugelius, G., Knoblauch, C., Romanovsky, V.,  
686 Schädel, C., Schneider von Deimling, T., Schuur, E. A. G., Shmelev, D., Ulrich, M. and Veremeeva, A.:  
687 Deep Yedoma permafrost: A synthesis of depositional characteristics and carbon vulnerability, *Earth-*  
688 *Science Rev.*, 172, 75–86, doi:10.1016/j.earscirev.2017.07.007, 2017.
- 689 Treat, C. C., Natali, S. M., Ernakovich, J., Iversen, C. M., Lupascu, M., McGuire, A. D., Norby, R. J., Roy  
690 Chowdhury, T., Richter, A., Šantrůčková, H., Schädel, C., Schuur, E. A. G., Sloan, V. L., Turetsky, M. R.  
691 and Waldrop, M. P.: A pan-Arctic synthesis of CH<sub>4</sub> and CO<sub>2</sub> production from anoxic soil incubations,  
692 *Glob. Chang. Biol.*, 21(7), 2787–2803, doi:10.1111/gcb.12875, 2015.
- 693 Ulrich, M., Grosse, G., Strauss, J. and Schirrmeister, L.: Quantifying wedge-ice volumes in Yedoma and  
694 thermokarst Basin deposits, *Permafr. Periglac. Process.*, 25(3), 151–161, doi:10.1002/ppp.1810, 2014.
- 695 Vonk, J. E., Sánchez-García, L., van Dongen, B. E., Alling, V., Kosmach, D., Charkin, A., Semiletov, I.  
696 P., Dudarev, O. V., Shakhova, N., Roos, P., Eglinton, T. I., Andersson, A. and Gustafsson, Ö.: Activation  
697 of old carbon by erosion of coastal and subsea permafrost in Arctic Siberia, *Nature*, 489(7414), 137–  
698 140, doi:10.1038/nature11392, 2012.
- 699 Waldrop, M. P., Wickland, K. P., White III, R., Berhe, A. A., Harden, J. W. and Romanovsky, V. E.:  
700 Molecular investigations into a globally important carbon pool: Permafrost-protected carbon in Alaskan  
701 soils, *Glob. Chang. Biol.*, 16(9), 2543–2554, doi:10.1111/j.1365-2486.2009.02141.x, 2010.
- 702 Walter Anthony, K. M., Zimov, S. A., Grosse, G., Jones, M. C., Anthony, P. M., Chapin III, F. S., Finlay,  
703 J. C., Mack, M. C., Davydov, S., Frenzel, P. and Frohling, S.: A shift of thermokarst lakes from carbon  
704 sources to sinks during the Holocene epoch, *Nature*, 511(7510), 452–456, doi:10.1038/nature13560,  
705 2014.
- 706 Walz, J., Knoblauch, C., Böhme, L. and Pfeiffer, E.-M.: Regulation of soil organic matter decomposition  
707 in permafrost-affected Siberian tundra soils - Impact of oxygen availability, freezing and thawing,  
708 temperature, and labile organic matter, *Soil Biol. Biochem.*, 110, 34–43,  
709 doi:10.1016/j.soilbio.2017.03.001, 2017.
- 710 Walz, J., Knoblauch, C., Tigges, R., Opel, T., Schirrmeister, L. and Pfeiffer, E.-M.: Incubation results  
711 from ice-rich permafrost deposits in Northeast Siberia, *PANGAEA*, doi:10.1594/PANGAEA.892950,  
712 2018.
- 713 Weiss, N., Blok, D., Elberling, B., Hugelius, G., Jørgensen, C. J., Siewert, M. B. and Kuhry, P.:  
714 Thermokarst dynamics and soil organic matter characteristics controlling initial carbon release from  
715 permafrost soils in the Siberian Yedoma region, *Sediment. Geol.*, 340, 38–48,  
716 doi:10.1016/j.sedgeo.2015.12.004, 2016.
- 717 Wetterich, S., Kuzmina, S., Andreev, A. A., Kienast, F., Meyer, H., Schirrmeister, L., Kuznetsova, T. and  
718 Sierralta, M.: Palaeoenvironmental dynamics inferred from late Quaternary permafrost deposits on  
719 Kurungnakh Island, Lena Delta, Northeast Siberia, Russia, *Quat. Sci. Rev.*, 27(15–16), 1523–1540,  
720 doi:10.1016/j.quascirev.2008.04.007, 2008.
- 721 Wetterich, S., Schirrmeister, L., Andreev, A. A., Pudenz, M., Plessen, B., Meyer, H. and Kunitsky, V. V.:  
722 Eemian and Late Glacial/Holocene palaeoenvironmental records from permafrost sequences at the  
723 Dmitry Laptev Strait (NE Siberia, Russia), *Palaeogeogr. Palaeoclimatol. Palaeoecol.*, 279(1–2), 73–95,  
724 doi:10.1016/j.palaeo.2009.05.002, 2009.
- 725 Wetterich, S., Rudaya, N., Tumskey, V., Andreev, A. A., Opel, T., Schirrmeister, L. and Meyer, H.: Last

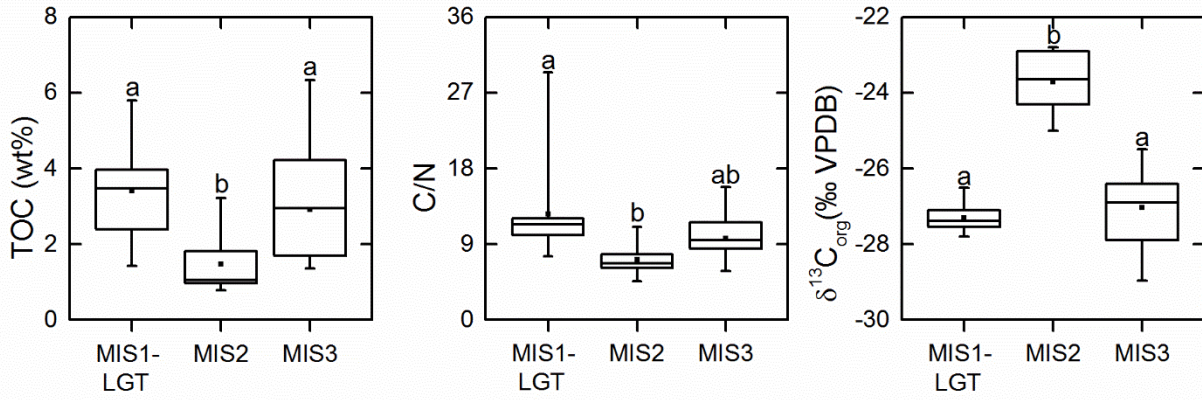
- 726 Glacial Maximum records in permafrost of the East Siberian Arctic, *Quat. Sci. Rev.*, 30(21–22), 3139–  
727 3151, doi:10.1016/j.quascirev.2011.07.020, 2011.
- 728 Wetterich, S., Tumskey, V., Rudaya, N., Andreev, A. A., Opel, T., Meyer, H., Schirrmeister, L. and Hüls,  
729 M.: Ice Complex formation in arctic East Siberia during the MIS3 Interstadial, *Quat. Sci. Rev.*, 84, 39–  
730 55, doi:10.1016/j.quascirev.2013.11.009, 2014.
- 731 Wetterich, S., Tumskey, V., Rudaya, N., Kuznetsov, V., Maksimov, F., Opel, T., Meyer, H., Andreev, A.  
732 A. and Schirrmeister, L.: Ice Complex permafrost of MIS5 age in the Dmitry Laptev Strait coastal region  
733 (East Siberian Arctic), *Quat. Sci. Rev.*, 147, 298–311, doi:10.1016/j.quascirev.2015.11.016, 2016.
- 734 Yamamoto, S., Alcauskas, J. B. and Crozier, T. E.: Solubility of methane in distilled water and seawater,  
735 *J. Chem. Eng. Data*, 21(1), 78–80, doi:10.1021/je60068a029, 1976.
- 736 Zimmermann, H., Raschke, E., Epp, L., Stoof-Leichsenring, K., Schirrmeister, L., Schwamborn, G. and  
737 Herzschuh, U.: The history of tree and shrub taxa on Bol'shoy Lyakhovsky Island (New Siberian  
738 Archipelago) since the last interglacial uncovered by sedimentary ancient DNA and pollen data, *Genes*  
739 (Basel), 8(10), 273, doi:10.3390/genes8100273, 2017a.
- 740 Zimmermann, H. H., Raschke, E., Epp, L. S., Stoof-Leichsenring, K. R., Schwamborn, G., Schirrmeister,  
741 L., Overduin, P. P. and Herzschuh, U.: Sedimentary ancient DNA and pollen reveal the composition of  
742 plant organic matter in Late Quaternary permafrost sediments of the Buor Khaya Peninsula (north-  
743 eastern Siberia), *Biogeosciences*, 14(3), 575–596, doi:10.5194/bg-14-575-2017, 2017b.
- 744 Zimov, S. A., Davydov, S. P., Zimova, G. M., Davydova, A. I., Schuur, E. A. G., Dutta, K. and Chapin III,  
745 F. S.: Permafrost carbon: Stock and decomposability of a globally significant carbon pool, *Geophys. Res.*  
746 *Lett.*, 33(20), L20502, doi:10.1029/2006GL027484, 2006.
- 747



749

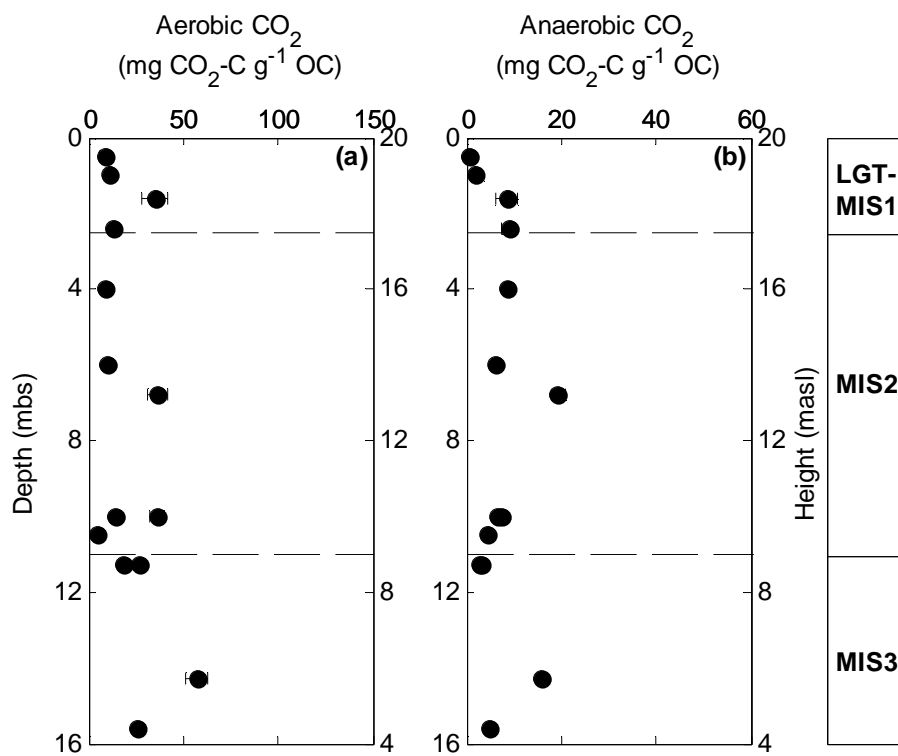
750 Figure 1. Overview map of the Laptev Sea region with the study locations at Muostakh Island (sample  
 751 code MUO12), the Buor Khaya Peninsula (BK8) and Bol'shoy Lyakhovsky Island (L14).

752



754

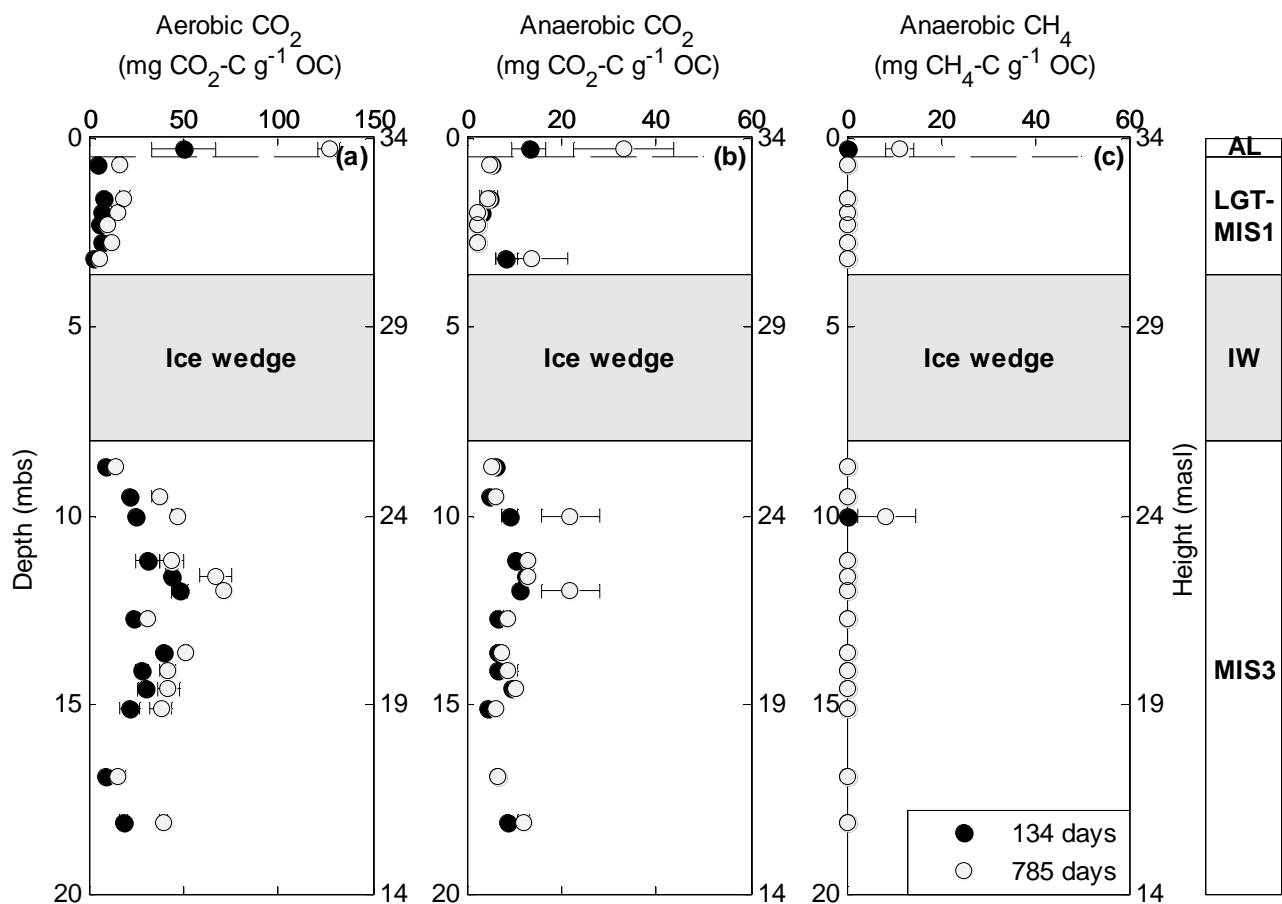
755 Figure 2. Boxplot of total organic carbon (TOC), total organic carbon to total nitrogen ratio (C/N) and  
 756  $\delta^{13}C_{org}$ -values of permafrost deposits from the MUO12 sequence, the BK8 core, and the two L14 cores  
 757 from the Holocene interglacial (MIS 1), including the late glacial transition (LGT) (n = 12), the Sartan  
 758 stadial (MIS 2) (n = 6), and the Kargin interstadial (MIS 3) (n = 27). The whiskers show the data range  
 759 and the box indicates the interquartile range. The vertical line and square inside the boxes show the  
 760 median and mean, respectively. The letters above the whiskers indicate statistically significant  
 761 differences in geochemical characteristics between the deposits of different ages (Mann-Whitney test, p  
 762 < 0.016 for TOC and C/N, p < 0.001 for  $\delta^{13}C_{org}$ )  
 763



764

765 Figure 3. Depth profiles of total aerobic (a) and anaerobic (b) CO<sub>2</sub> production per gram organic carbon  
 766 (g<sup>-1</sup> OC) in sediment samples from the MUO12 sequence after 134 incubation days at 4 °C for deposits  
 767 from the Holocene interglacial (MIS 1), including the late glacial transition (LGT), the Sartan stadial (MIS  
 768 2), and the Kargin interstadial (MIS 3). Data are mean values (n = 3) and error bars represent one  
 769 standard deviation. Note the different scales. No CH<sub>4</sub> production was observed during the 134-days  
 770 incubation period.

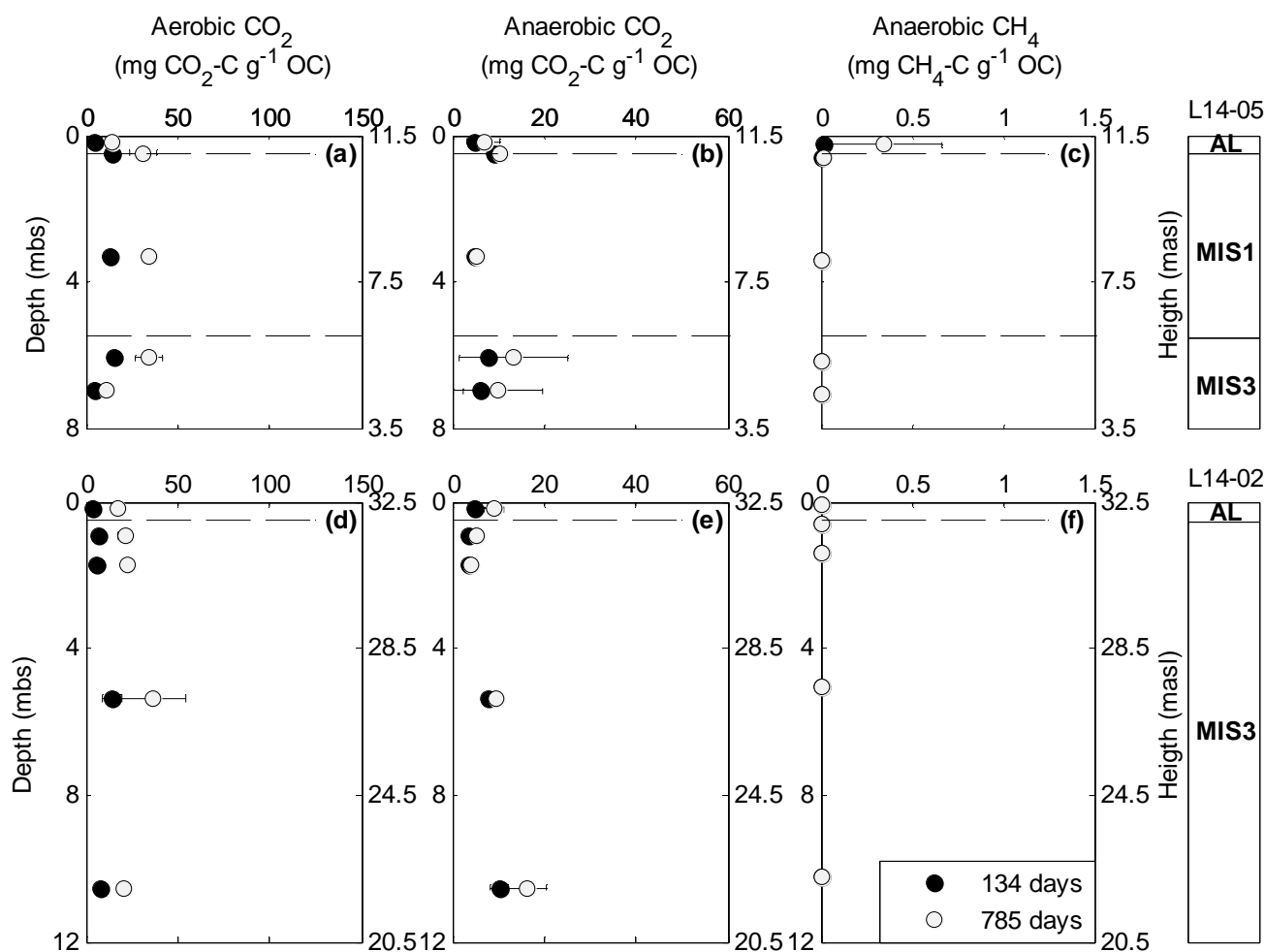
771



772

773 Figure 4. Depth profiles of total aerobic CO<sub>2</sub> (a), anaerobic CO<sub>2</sub> (b) and anaerobic CH<sub>4</sub> (c) production  
 774 per gram organic carbon (g<sup>-1</sup> OC) in sediment samples from the BK8 core after 134 (closed symbols)  
 775 and 785 incubation days (open symbols) at 4 °C for the active layer (AL), which is considered to be 0.5  
 776 m thick, and permafrost deposits from the Holocene interglacial (MIS 1), including the late glacial  
 777 transition (LGT) and the Kargin interstadial (MIS 3). Data are mean values (n = 3) and error bars  
 778 represent one standard deviation. Note the different scales.

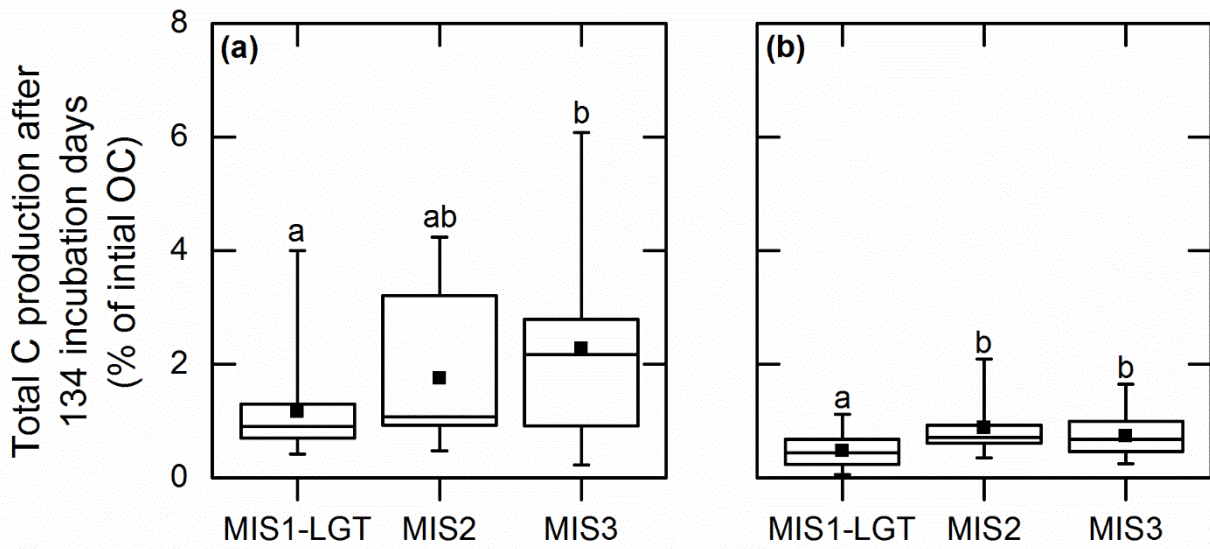
779



780

781 Figure 5. Depth profiles of total aerobic CO<sub>2</sub> (a), anaerobic CO<sub>2</sub> (b) and anaerobic CH<sub>4</sub> (c) production  
 782 per gram organic carbon (g<sup>-1</sup> OC) in sediment samples from the L14-05 (a,b,c), and L14-02 cores (d,e,f)  
 783 after 134 (closed symbols) and 785 incubation days (open symbols) at 4 °C for the active layer (AL),  
 784 which is considered to be 0.5 m thick, and permafrost deposits from the Holocene interglacial (MIS 1)  
 785 and the Kargin interstadial (MIS 3). Data are mean values (n = 3) and error bars represent one standard  
 786 deviation. Note the different scales.

787



788

789 Figure 6. Total aerobic (a) and anaerobic (b) CO<sub>2</sub>-C production after 134 incubation days from permafrost  
 790 deposits from the MUO12 sequence, the BK8 core, and the two L14 cores from the Holocene interglacial  
 791 (MIS 1), including the late glacial transition (LGT) (n = 22), the Sartan stadial (MIS 2) (n = 15), and the  
 792 Kargin interstadial (MIS 3) (n = 50). The whiskers show the data range and the box indicates the  
 793 interquartile range. The vertical line and square inside the boxes show the median and mean,  
 794 respectively. The different letters indicate significant differences (Mann-Whitney test, p < 0.016) between  
 795 deposits from different periods.

796

797 **Tables**

798 Table 1. Compilation of the regional chronostratigraphy of the Laptev Sea region used in this work with  
 799 paleoclimate (summer) and vegetation history based on an overview by Andreev et al. (2011) and  
 800 references therein.

Age	Period	Regional chrono-stratigraphy	Marine Isotope Stage (MIS)	Regional climate and vegetation
ka BP				
<10.3	Holocene	Holocene	MIS 1	Climate amelioration during the early Holocene; shrub-tundra vegetation gradually disappeared ca 7.6 ka BP
ca 10.3–13	Late glacial-early Holocene transition			Climate amelioration after the Last Glacial Maximum; transition to shrubby tundra vegetation
ca 13–30	Late Weichselian glacial (stadial)	Sartan	MIS 2	Cold and dry summer conditions, winter colder than today; open tundra steppe
ca 30–55	Middle Weichselian glacial (interstadial)	Kargin	MIS 3	Relatively warm and wet summers; open herb and shrub dominated vegetation

801

802 [Table 2. Mean \( \$\pm\$  one standard deviation\) CO<sub>2</sub> and CH<sub>4</sub> production after 134 and 785 incubation days.](#)  
 803 [Production after 785 days was not determined \(n.d.\) for the Muostakh Island sequence. MIS 2 deposits](#)  
 804 [were not present in the sample material from the Buor Khaya Peninsula and Bol'shoy Lyakhovsky Island.](#)

<a href="#">Location (sample code)</a>	<a href="#">Marine Isotope Stage (MIS)</a>	<a href="#">n</a>	<a href="#">Aerobic CO<sub>2</sub> production (mg CO<sub>2</sub>-C g<sup>-1</sup> OC)</a>		<a href="#">Anaerobic CO<sub>2</sub> production (mg CO<sub>2</sub>-C g<sup>-1</sup> OC)</a>		<a href="#">Anaerobic CH<sub>4</sub> production (mg CH<sub>4</sub>-C g<sup>-1</sup> OC)</a>	
			<a href="#">134 days</a>	<a href="#">785 days</a>	<a href="#">134 days</a>	<a href="#">785 days</a>	<a href="#">134 days</a>	<a href="#">785 days</a>
<a href="#">Muostakh Island (MUO12)</a>	<a href="#">Active layer</a>	<a href="#">Not sampled</a>						
	<a href="#">MIS 1</a>	<a href="#">12</a>	<a href="#">17.0 <math>\pm</math> 11.9</a>	<a href="#">n.d.</a>	<a href="#">4.9 <math>\pm</math> 4.2</a>	<a href="#">n.d.</a>	<a href="#">0</a>	<a href="#">n.d.</a>
	<a href="#">MIS 2</a>	<a href="#">17</a>	<a href="#">17.4 <math>\pm</math> 12.9</a>	<a href="#">n.d.</a>	<a href="#">8.8 <math>\pm</math> 5.2</a>	<a href="#">n.d.</a>	<a href="#">0</a>	<a href="#">n.d.</a>
	<a href="#">MIS 3</a>	<a href="#">12</a>	<a href="#">32.2 <math>\pm</math> 15.6</a>	<a href="#">n.d.</a>	<a href="#">6.6 <math>\pm</math> 5.6</a>	<a href="#">n.d.</a>	<a href="#">0</a>	<a href="#">n.d.</a>
<a href="#">Buor Khaya Peninsula (BK8)</a>	<a href="#">Active layer</a>	<a href="#">3</a>	<a href="#">50.2 <math>\pm</math> 16.9</a>	<a href="#">126.8 <math>\pm</math> 6.0</a>	<a href="#">13.3 <math>\pm</math> 3.5</a>	<a href="#">33.1 <math>\pm</math> 10.6</a>	<a href="#">0.4 <math>\pm</math> 0.2</a>	<a href="#">11.4 <math>\pm</math> 3.0</a>
	<a href="#">MIS 1-LGT</a>	<a href="#">15</a>	<a href="#">6.1 <math>\pm</math> 1.8</a>	<a href="#">13.4 <math>\pm</math> 4.5</a>	<a href="#">4.1 <math>\pm</math> 2.2</a>	<a href="#">4.5 <math>\pm</math> 4.1</a>	<a href="#">0</a>	<a href="#">0</a>
	<a href="#">MIS 2</a>	<a href="#">Not present in the core material</a>						
	<a href="#">MIS 3</a>	<a href="#">38</a>	<a href="#">27.2 <math>\pm</math> 11.7</a>	<a href="#">42.2 <math>\pm</math> 15.9</a>	<a href="#">7.9 <math>\pm</math> 2.5</a>	<a href="#">11.0 <math>\pm</math> 5.8</a>	<a href="#">0</a>	<a href="#">0.4 <math>\pm</math> 2.1 *</a>
<a href="#">Bol'shoy Lyakhovsky Island (L14)</a>	<a href="#">Active layer</a>	<a href="#">6</a>	<a href="#">4.3 <math>\pm</math> 0.6</a>	<a href="#">15.9 <math>\pm</math> 2.8</a>	<a href="#">5.0 <math>\pm</math> 1.3</a>	<a href="#">8.0 <math>\pm</math> 2.7</a>	<a href="#">0</a>	<a href="#">0.2 <math>\pm</math> 0.3 *</a>
	<a href="#">MIS 1-LGT</a>	<a href="#">6</a>	<a href="#">13.8 <math>\pm</math> 2.4</a>	<a href="#">32.6 <math>\pm</math> 4.8</a>	<a href="#">6.9 <math>\pm</math> 2.3</a>	<a href="#">7.8 <math>\pm</math> 2.9</a>	<a href="#">0</a>	<a href="#">0</a>
	<a href="#">MIS 2</a>	<a href="#">Not present in the core material</a>						
	<a href="#">MIS 3</a>	<a href="#">18</a>	<a href="#">9.2 <math>\pm</math> 4.7</a>	<a href="#">24.7 <math>\pm</math> 11.1</a>	<a href="#">6.6 <math>\pm</math> 2.9</a>	<a href="#">9.7 <math>\pm</math> 7.0</a>	<a href="#">0</a>	<a href="#">0</a>

805 \* Methanogenesis was only observed in two out of three replicates